

---

# PRIVACY-PRESERVING GENERATIVE MODELS: A COMPREHENSIVE SURVEY

---

**Debalina Padariya**

School of Computer Science and Informatics  
De Montfort University  
Leicester, United Kingdom  
p2723446@my365.dmu.ac.uk

**Isabel Wagner**

Department of Mathematics and Computer Science  
University of Basel  
Basel, Switzerland  
isabel.wagner@unibas.ch

**Aboozar Taherkhani**

School of Computer Science and Informatics  
De Montfort University  
Leicester, United Kingdom  
aboozar.taherkhani@dmu.ac.uk

**Eerke Boiten**

School of Computer Science and Informatics  
De Montfort University  
Leicester, United Kingdom  
eerke.boiten@dmu.ac.uk

February 7, 2025

## ABSTRACT

Despite the generative model's groundbreaking success, the need to study its implications for privacy and utility becomes more urgent. Although many studies have demonstrated the privacy threats brought by GANs, no existing survey has systematically categorized the privacy and utility perspectives of GANs and VAEs. In this article, we comprehensively study privacy-preserving generative models, articulating the novel taxonomies for both privacy and utility metrics by analyzing 100 research publications. Finally, we discuss the current challenges and future research directions that help new researchers gain insight into the underlying concepts.

## 1 Introduction

In recent years, the demand for generating valuable insights on applications while maintaining the privacy of individuals has increased. Synthetic data generation (SDG) is one of the emerging use cases of generative AI and has made significant progress as a privacy-enhancing technology [11]. SDG aims to closely resemble real-world data, maintaining data privacy while preserving sufficient usefulness for analysis. Since the limitations of traditional de-identification methods are more evident, there is growing attention to SDG that captures the underlying distributions of real data. Although synthetic data holds great promise in multiple sectors, it is not a case of "Fake it till you make it" [94]. The potential privacy attacks associated with generative models emerge as critical issues [94, 111]. Therefore, despite its promise for privacy-preserving data publishing, SDG requires adherence to regulations like GDPR, which restrict the collection and use of real data [38].

Privacy-preserving generative models can address these challenges by releasing realistic synthetic samples [105, 16]. The popular approach is differential privacy (DP), which holds great promise for quantifying the privacy risk [29]. However, DP is unlike having a "rich, calorie-free cake," and the trade-offs between privacy and utility are complex [37]. There are many approaches for creating synthetic data with machine learning-based models, such as Generative Adversarial Networks (GANs), Variational Autoencoders (VAEs), statistical-based Gaussian Copula, transformer-based and agent-based models, or other ML-based methods [72]. This paper primarily focuses on the leading generative models, such as GANs and VAEs, which show remarkable performance in producing high-quality realistic synthetic samples [6].

## 1.1 Background

Generative models have gained significant attention for unsupervised learning in a broad range of applications, such as image generation [6, 89], tabular data synthesis [63, 108], time-series data generation [33, 10], natural language processing [91], and audio/video generation [75]. Goodfellow et al. [40] first proposed the GANs framework, which involves two neural networks competing in a minimax game. A generator network uses a random noise vector to generate new samples by learning the real data distribution. In contrast, a discriminator network works as a classification model to distinguish between real and generated samples. Many GAN variants have been proposed over the past few years, focusing on two objectives: improving training stability and deploying GANs for real-world applications [89, 78, 6, 41, 56]. Knigam and Welling [59] introduced VAEs, recognized as popular likelihood-based models. VAEs are associated with autoencoders comprising two interconnected networks: an encoder and a decoder. The encoder network takes the initial feature representation as input and transforms it into a dense representation. Conversely, the decoder network is trained to reconstruct the original data from the encoded representation. A latent space or bottleneck consists of the compressed representation of the input data. Reconstruction loss measures how well a model reconstructs original data from its encoded form. The primary benefit of VAEs is their ability to control latent distributions, improving sample quality, but sometimes they can produce blurry outputs [76].

Despite the widespread success of generative models in various applications, several privacy threats have emerged as a significant concern [17, 44, 94] and privacy-preserving generative models have experienced rapid development in the past few years. DP provides a theoretical privacy guarantee through a noise-adding mechanism [29]. In DP, the privacy parameters  $\epsilon$  and  $\delta$  quantify privacy loss by measuring the noise added to data. The pure DP mechanism, or  $\epsilon$ -DP, ensures that the output distribution remains almost identical for any two datasets that differ by at most one record. In approximate DP ( $\epsilon, \delta$ -DP),  $\epsilon$  controls privacy, while  $\delta$  represents the probability that the privacy guarantee might be violated. Differential privacy mechanisms have two key properties. First, composition refers to the joint distribution of the output of differentially private mechanisms that satisfy DP. Second, post-processing indicates that without additional knowledge of the private database, the function of the output of the differentially private algorithm can not be computed.

## 1.2 Scope and Motivation

Some literature surveys have been published in the last few years on privacy aspects of generative models. Fan [30] provides a short review of existing approaches of differentially private GANs while emphasizing their evaluation metrics and application domains. However, this survey excludes the state-of-the-art privacy approaches in other generative models, e.g., VAEs, and only a limited number of differential privacy approaches applied to GANs. Additionally, privacy-preserving generative models have evolved over the past five years with effective noise-adding mechanisms in DP. Cai et al. [15] break down the GAN's privacy approaches into data and model-level while comparing the GAN-based security issues across different application areas. Although they cover different privacy metrics with a wide range of applications, the study lacks an in-depth analysis of them, covering only GAN-based privacy and security issues. Some surveys [95, 112] briefly overview adversarial attacks in generative models while focusing only on attack-based privacy metrics, with a lack of guidance in identifying suitable metrics to maximize the benefits of generative models. Moreover, to our knowledge, no research has been conducted focusing on utility metrics in generative models. We address this gap by presenting our work, which seeks to provide the latest research around privacy and utility metrics with extended taxonomies and critically review the pros and cons of selecting particular metrics. We systematically analyze an exhaustive list of publications from top-tier conferences and digital sources. To achieve these objectives, the following research questions are addressed:

RQ1: What are the privacy attacks associated with generative models?

RQ2: What are the approaches to quantifying privacy in generative models?

RQ3: How can the utility of generative models be assessed?

RQ4: What are the open gaps and challenges in privacy-preserving generative models?

## 1.3 Contribution

Our contribution aims to comprehensively review the state-of-the-art privacy and utility metrics associated with generative models. This survey offers a deeper discussion of these concepts, categorization with several taxonomies, and insights into the open gaps and challenges with future research directions. The main contributions of this article are:

- **Comprehensive Review:** This study comprehensively reviews the literature on privacy-preserving generative models. This is an in-depth analysis of over 100 research papers. To the best of our knowledge, this is the first work to provide a detailed comparison of both privacy and utility metrics.

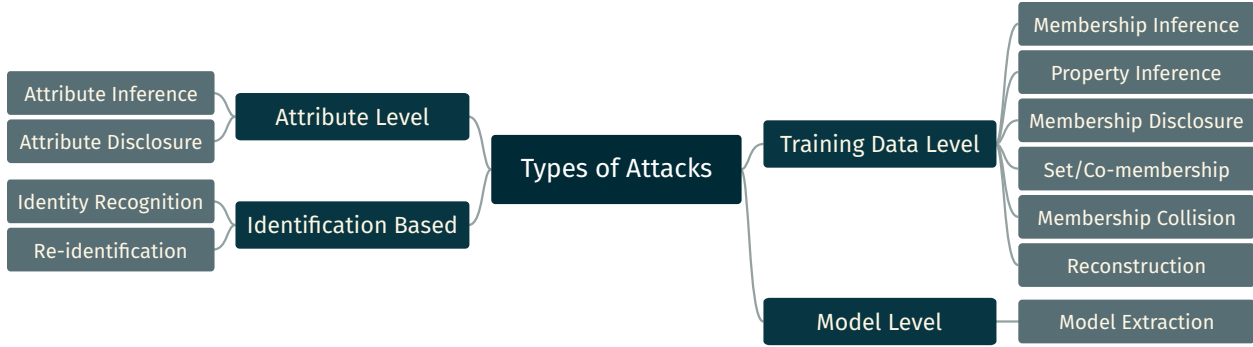


Figure 1: Types of Privacy Attacks in Generative Models

- **Taxonomies of Privacy and Utility Metrics:** There have been various privacy and utility metrics used in the current landscape of generative models — it is challenging and time-intensive to understand the broad picture of all works within this field. To offer readers a more accessible means of understanding existing studies, we provide novel taxonomies to categorize privacy and utility metrics of generative models. These taxonomies allow the reader to understand the similarities and differences of various metrics. We have provided taxonomies of privacy attacks in support of this and their adversarial assumptions against generative models.
- **Open Gaps and Challenges:** We elicit objectives for future research by assessing the state-of-the-art against the research questions posed. Based on the literature reviewed, we shed light on the challenges yet to be solved and propose several promising future directions.

The rest of the article is structured as follows: Section 2 reviews the potential privacy attacks associated with generative models. Based on the proposed taxonomies, we review and discuss generative models’ privacy and utility metrics in Section 3 and Section 4. We conclude our survey in Section 5 by providing open challenges and future research directions.

## 2 Attacks on Generative Models

The effects of attacks on the generation model are gaining more attention. Many studies have shown that generative models are vulnerable to attacks that break a model’s integrity by disrupting the model’s generation capacity or privacy by inferring sensitive information about the target model. This survey focuses on privacy attacks, where the vulnerability to attacks depends on the attack types and strategies (Section 2.1) and the attacker’s assumption about the target model. It is the adversary’s prior knowledge of the target model, such as training data distributions, model parameters, model structure, latent code, or generated samples. Based on the attacker’s assumption, privacy attacks can be classified into two groups: Black-Box attacks and White-Box attacks. In full black-box attacks, the adversary can only access the synthetic samples from generative models [94, 51], whereas in the partial black-box settings, the attacker may access partial knowledge of the target model, such as partial real training data or latent code of the target model [44, 17]. On the other hand, in white-box settings, the attacker has some knowledge about the model, such as the training algorithm, model parameters, model architecture, or its original training data, such as partial or full training data distributions [50, 17, 87, 82].

### 2.1 Types of Privacy Attacks

The attacker aims to gain information that is not intended to be shared, such as information about the training data and attributes, the target model, or specific instances. The components of GANs and VAEs, such as the latent code, generator, discriminator, encoder, or decoder, are vulnerable to such attacks. This section categorizes privacy attacks into four types (see Figure 1): training data level, attribute level, model level, and identification-based.

#### 2.1.1 Training Data Level

At the training data level, the adversary aims to infer information about training data samples. For instance, if a model is trained on the genetic data of cancer patients, an adversary can infer individual cancer status or specific gene details of all patients. Hence, we classify the training data-level privacy attacks into five categories: membership inference, property inference, membership disclosure, co-membership, and reconstruction.

**Membership Inference Attacks (MIA)** MIA is the most well-known privacy attack [93]. In MIA, the attacker tries to determine whether an input sample  $x$  is part of a training dataset  $D$ . A common MIA strategy is to build a local shadow model to mimic the target model and then manipulate the model. The idea is to gain more knowledge of the target model by building multiple shadow models. Because the output of the shadow models provides a prediction vector, it is useful to predict the membership in the training samples. The strategy behind shadow model training is related to overfitting, where a model works well on the training set but not on unseen data. Besides, shadow model training-based MIA against generative models [106, 33, 88, 85, 110, 49], variants of MIA also include distance-based MIA [46, 17] and representation learning-based MIA [115].

**Property Inference Attacks** These attacks attempt to infer a generic property of the training dataset from a target model [117]. The adversary queries the target model to achieve synthetic samples and then trains a property classifier to label these samples to infer the target property. In that case, the adversary can use shadow model training, using an auxiliary dataset to train the property classifier. Property inference attacks can serve as the backbones for other attacks, i.e., membership inference attacks.

**Membership Disclosure** Through a membership disclosure attack, the attacker aims to identify an individual in the private dataset correctly, such as accessing a private patient record for model training. Some researchers describe membership disclosure by accessing partial or complete sets of training samples [39, 24]. The intuition is that if a record is used to train the generative model, at least one synthetic sample is within a certain distance from the record. For instance, they use Hamming distance to compute the distance of each record to each sample from the synthetic dataset, where the attacker successfully identifies the records used for training at a smaller distance.

**Set-membership/Co-membership Attacks** For set-membership, the adversary aims to identify whether a given set of records is used in the training set. Hilprecht et al. [46] describe a set membership attack with the perspective of regulatory audits to prove data privacy violations, i.e., certain records are illegally used to train a generative model. To perform a set membership attack, the adversary holds some prior information, such as to which data source the samples belong, i.e., training or testing. First, this study launches single membership inference using these samples and then sorts the results with the distance function. Second, the top samples are recorded as a part of the training data.

In another study, Liu et al. [68] perform co-membership attacks to identify whether all or none of the samples are used in the training set, e.g., multiple photos uploaded from a mobile. This study designs this attack against GANs and VAEs in two scenarios. First, the adversary mounts single membership inference on target samples by optimizing it using an attacker network. Second, the attacker network finds an optimal latent code using the query sample input. In that case, the adversary combines target samples to guide the attacker network in a co-membership attack, leveraging shared membership status to determine the final co-membership.

**Membership Collision** This attack retrieves partial real training samples by accessing randomly sampled synthetic queries. Hu et al. [49] propose membership collision attacks against GANs using synthesized tabular data. In tabular data, synthetic tables often overlap with the GAN's training samples, leading to a privacy violation if an adversary detects this intersection. They define this intersection as a membership collision. To perform this attack, this study uses a shadow model to train an attack model that predicts the collision probability of synthetic samples. Moreover, their findings show a positive relationship between membership collision and sample frequency, reflected as an indicator of membership collision.

**Reconstruction Attacks** In this scenario, the adversary attempts to reconstruct one or more training samples. This is also called a model inversion attack, introduced by Fredrikson et al. [32], where the adversary tries to recover the full data sample or its sensitive features. To investigate this attack, this study exploits a machine learning model's confidence score to analyze patterns and infer sensitive training data features. They use a face recognition system to reconstruct faces by training face classifiers using a linear regression model. Inspired by this approach, Li et al. [66] perform a reconstruction attack against GANs for a face recognition system.

### 2.1.2 Attribute Level

At the attribute level, the attacker tries to infer sensitive features of the attributes of individual training data, such as race, gender, or medical test results.

**Attribute Inference Attacks** In this attack, the attacker attempts to predict the values of sensitive attributes by accessing the generative models. It is also referred to as linkage attacks, where the adversary tries to link specific sensitive attributes with a given data entry. Stadler et al. [94] perform an attribute inference attack against GANs by

developing an attribute inference game where the adversary can access the generated and partial real training samples. The idea is the adversary tries to predict an unknown attribute from known ones and then tries to infer the missing value via record linkage. If he succeeds in the linkage based on the known attributes, he reconstructs missing sensitive attributes; otherwise, the adversary uses the publicly released data to predict sensitive values. Inspired by this approach, several studies conduct attribute inference attacks against GANs [48, 62].

**Attribute Disclosure** This refers to the risk of an attacker correctly identifying the sensitive attributes of a target record based on the known attributes of real training samples. For example, the adversary can learn unknown attributes in a healthcare database by observing similar patient records. Some researchers describe attribute disclosure risk against GANs [24, 39]. To perform this, they consider  $k$  - nearest neighboring distance, where the adversary can extract  $k$  - nearest neighbor of the generated samples based on the known attributes achieved from the compromised record.

### 2.1.3 Model Level

At the model level, the adversary tries to take information from the target model and replicate the model.

**Model Extraction Attacks** In this scenario, the adversary attempts to replicate the full model by extracting information with the intention that the substitute model matches the target model's accuracy. Hu et al. [50] propose a model extraction attack against GANs. This study proposes an attack model for accuracy-based extraction aiming to steal the data distributions of the target model, i.e., generated and training data distributions. The strategy is querying the publicly released target model to gain the generated samples and then build a local copy of the target model. Additionally, to improve the attacker's effectiveness, they perform a fidelity-based extraction strategy, which involves two scenarios: accessing partial real-trained data in partial black-box settings and accessing the discriminator of the target model in white-box settings.

### 2.1.4 Identification Based

In this scenario, the attacker attempts to recognize an individual identity based on their patterns, features, or characteristics. Alternatively, the attacker can re-identify individuals from an anonymized dataset.

**Identity Recognition Attacks** Identity recognition identifies external entities' identity based on specific features or characteristics, i.e., face identification in face recognition systems. This occurs at the training data level, attribute, or feature level. For instance, pattern analysis in medical images happens at the training data level, while face identification focuses on specific attributes at the feature level. Chen et al. [20] propose three threat scenarios to show the effectiveness of an identity recognition attacker for face recognition systems on VAEs and GANs. First, the adversary can target the unaltered training dataset and privacy-protected test dataset. Second, the attacker can access private training data to obtain the underlying ground truth identities and then train the identifier on training images, which consist of the same target identity as test images. In the last scenario, the attacker can retrieve the latent vector representations by controlling the encoder network.

Croft et al. [25] explore identity recognition attacks for facial obfuscation against GANs by a parrot attack. During training, a parrot attack employs a neural network to classify identities by using labeled samples of obfuscated images in the training set, learning the identification pattern through the process. In another study, Liu et al. [67] describe identifying facial expressions in synthetic data against GANs. This study designs an adversarial approach, e.g., a steganography-based attack strategy, to understand how the adversary can extract sensitive attributes from input images, such as facial expressions. For instance, the adversary can extract sensitive information through the fully connected neural network layers to understand latent vectors, which helps to learn the feature representations of input in performing an identity recognition attack.

**Re-identification Attacks** In this scenario, the attacker reveals the identity of a target record by linking it with some known information about the target record. Two types of identifying attributes increase the risk of re-identification. First, identifying attributes directly linked to an individual's identity, such as phone number or email address. Second is quasi-identifying attributes, which can be combined with other quasi-identities for re-identification attacks, i.e., date of birth, zip code, gender, etc. Yoon et al. [111] analyze re-identification risk for patient data against GANs. For example, re-identification risk increases if a patient's date of hospital visits or medical procedures is combined with other attributes. Gafni et al. [34] describe re-identification risk against GANs for video applications. In this study, the attacker can exploit the latent space representation to extract full information of an identity. In another study, Maximov et al. [74] consider re-identification risk for people in video and image streams against GANs. They examine whether the attacker controls the pose preservation process or the temporal consistency, such as stability and continuity of video processing, as this makes GANs susceptible to re-identification risk.

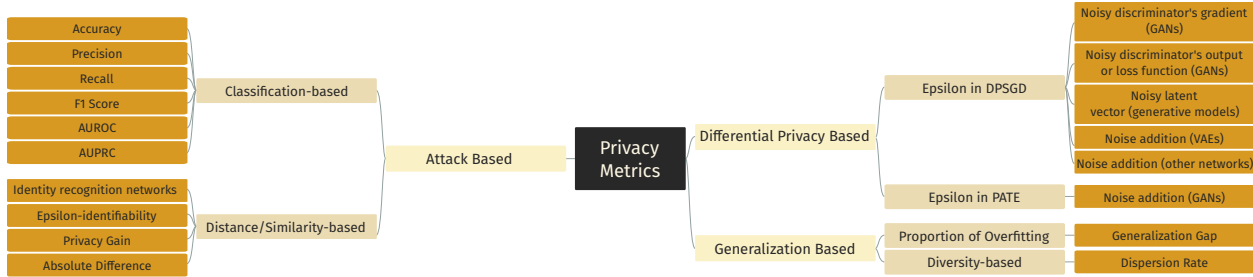


Figure 2: Taxonomy of Privacy Metrics in Generative Models

### 3 Privacy Metrics in Generative Models

Despite the generative model’s success, emerging privacy threats have led researchers to improve privacy protection in this field. This survey explores the progress of privacy metrics by showcasing different privacy measures and the wide range of privacy guarantees established by researchers. A generic approach is to use attack-based privacy metrics, where an attacker’s success rate measures the privacy of the target generative model [44, 17, 94]. Alternatively, researchers have pointed out the poor generalization properties of generative models, where the proportion of overfitting can be a factor that measures information leakage [21]. The approaches based on differential privacy, which integrate noise-adding mechanisms, provide insight into the overall privacy costs spent against generative models [105, 106, 100]. We propose a taxonomy of privacy metrics that allows categorizing different privacy measures, described in Figure 2.

#### 3.1 Attack based Metrics

In many approaches to privacy-preserving synthetic data, their privacy level is approached from the perspective of a specific attack. Many of these attacks return a value that may or may not be a valid result. Consequently, these attacks effectively present classification problems and their success; hence, the level of privacy can be measured based on confusion matrices. Others compare the distributions of original data and the outcomes of an attack on synthetic data. We summarize the metrics into two categories: classification-based and distance/similarity-based.

##### 3.1.1 Classification-based Metrics

This metric assesses how a classifier performs. The standard approach to evaluating the classifier’s quality is via a confusion matrix. This matrix shows true positive, true negative, false positive, and false negative results for binary classification problems. Different metrics, such as accuracy, precision, recall, and F1 score, are derived from the confusion matrix. Besides these, other classification metrics, such as AUROC (Area Under the Receiver Operating Characteristic Curve) or AUPRC (Area Under Precision-Recall Curve), are suitable for evaluating the classifier over all possible thresholds.

**Accuracy** This metric represents the percentage of accurately predicted instances compared to the total number of instances in a particular dataset. For instance, the accuracy of membership inference attacks represents how many correct predictions the attacker makes within all observations. Many studies use this metric to measure the membership inference success rate against generative models [44, 46, 87, 82, 20, 17]. Some factors can influence the accuracy, such as knowledge about the target generative model, training dataset size or the number of training epochs. For instance, the partial black box-based MIA with limited auxiliary knowledge [44] or knowledge about the latent code in white box settings [17, 46] achieve higher accuracy than full black box-based MIA [44]. Besides adversarial knowledge, some studies suggest that other factors, e.g., the size of training samples, can contribute to the success rate of MIA [44, 46, 17]. Since smaller training datasets lead to the model’s overfitting, it is highly likely to increase membership inference accuracy.

The accuracy of a model extraction attack shows how well the attacker replicates the target model’s behavior and performance [50]. The accuracy of an identity recognition attack indicates how effectively the attacker can correctly identify individuals within a given dataset or system. Liu et al. [67] consider the discriminator’s accuracy, where various factors can increase the discriminator’s accuracy, such as network architectures, optimization techniques, training dataset size, or the number of training epochs.

**Precision/Recall** Precision measures the ratio of correct positive predictions (true positives) among all positive predictions in classifying the data instances. The precision of membership inference represents the fraction of records

inferred that are indeed members of the training dataset. Alternatively, recall measures the ratio of correct positive instances (true positives) among all actual positive instances. For example, recall quantifies the fraction of the training dataset’s members correctly inferred as members by the membership adversary. Goncalves et al. [39] use precision to measure membership disclosure and attribute disclosure success rate, where the adversary chooses a Hamming distance of each sample from the synthetic dataset to each sample in the training dataset. The distance of 0 indicates high membership disclosure precision, indicating a high percentage of target records identified by the attacker. Conversely, a larger Hamming distance leads to higher recall, indicating the higher inclusion of target records in the training dataset. Regarding the success rate of these attacks, they report that the size of synthetic samples impacts recall with no effect on precision values.

Maximov et al. [74] measure re-identification risk using a standard recall metric for image anonymization against GANs. This metric counts the proportion of nearest neighbor samples of the same class ranging from 0 to 100, where 100 indicates a higher re-identification success rate. Additionally, a few works use a FaceNet identity recognition network to measure the success rate of identity recognition attacks against generative models [34, 74]. The FaceNet network uses a true acceptance rate (TAR), the ratio of true positive identifications to false positive identifications, where the network achieves a higher identification success rate with a true acceptance rate of almost 0.99.

**F1-Score** This is the harmonic mean of precision and recall. The F1 score of MIA represents a single measure of its effectiveness while identifying as many true members as possible and reducing the incorrectly identifying error of non-members. The F1 score is a better performance metric for imbalanced classes. Park et al. [88] use the F1 score to measure the success rate of membership inference and attribute disclosure with an imbalanced dataset. Since the F1 score balances precision and recall, a smaller F1 score indicates a declining proportion of correctly identifying members in membership inference or sensitive attributes of a target record in attribute disclosure. Besides, Hyeong et al. [51] use the aggregation method of F1 score, i.e., Macro F1 score, calculated as the average of F1 score across all classes in multi-class classification problems to estimate the membership adversary’s success rate.

**AUROC** An AUROC visually represents a model’s performance at different classification thresholds. This metric is used to evaluate binary classifiers, ranging from 0 to 1, where a value 0.5 represents a random guessing. The AUROC of membership inference indicates how well the attacker can distinguish between the two classes: members and non-members. Some researchers have used this metric to measure the success rate of membership inference and co-membership attacks for GANs and VAEs [68, 21]. Their findings indicate that the attacker’s AUROC score increases with the effective size of training samples and adversarial knowledge of the target model. Similarly, Park et al. [88] use the AUROC score to measure the MIA performance. Their findings suggest that improved quality of synthetic samples can produce more realistic cumulative distributions, resulting in a lower success rate of an attacker.

**AUPRC** This metric is derived as the area under the precision-recall curve, which shows the trade-off between them across various thresholds. The AUPRC of MIA indicates the attacker’s performance in identifying whether target individuals belong in the training dataset. AUPRC is more informative than AUROC for imbalanced data problems, i.e., where the negative class dominates, such as non-members, in membership inference. Since AUPRC measures how well the minority class is predicted, it gives less priority to false positives resulting from the majority class. Hu et al. [49] use this metric to estimate the success rate for membership collision attacks against GANs, where a higher AUPRC indicates that the attacker accurately identifies the training sample. They also report that training data size and number of epochs can enhance the adversary’s success rate. With the increasing training iterations, GANs learn more about the training data distribution, which enhances attack accuracy. In another study, Bernau et al. [12] use an average precision metric to estimate the performance of reconstruction membership attacks against VAEs. The average precision represents the weighted mean of precisions obtained at each threshold.

### 3.1.2 Distance/Similarity-based Metrics

These metrics are estimated between the distribution of the real and the synthetic samples, quantifying their dissimilarity. For instance, some studies have used these metrics to measure the privacy risks where the distribution of original data and the outcome of re-identification or identity recognition-based attacks on generative models estimate the level of privacy [80, 25]. Some identity recognition networks, such as FaceNet, ArcFace, and Siamese, particularly for facial recognition systems, measure the ability of the system to re-identify an individual across different datasets. Montenegro et al. [80] have adopted a Siamese identity recognition network, which defines a maximum identity score, indicating the highest degree of similarity to predict the identity of privatized samples. Besides, some researchers have used FaceNet identification networks to estimate the re-identification success rate for face anonymization against GANs [74, 25]. The FaceNet network uses a similarity threshold by comparing the distance of two faces, where a value smaller than a threshold expresses the same identity [92]. Besides, few studies prefer another face recognition network, ArcFace, to

measure the identification risks for facial images [34, 98]. ArcFace uses a deep convolutional neural network (CNN), where a distance metric, i.e., cosine distance, is used to find a similarity score to identify a potential match [26].

Yoon et al. [111] propose a similarity-based metric, i.e.,  $\epsilon$ -identifiability, to measure the re-identification risk against GANs for healthcare applications. The concept of identifiability is based on the fact that synthetic patient observations should differ enough from the original patient observations to ensure de-identification. They use a weighted Euclidean distance metric to measure the minimum distance between these two records. The  $\epsilon$ -identifiability defines a threshold with ( $\epsilon \in [0, 1]$ ), where 0-identifiability represents a perfect de-identification, and 1-identifiability implies perfect identification of a particular record. Besides, few studies have adopted the privacy gain metric, indicating a reduction in the adversary’s advantage [94, 84]. This metric is estimated as the difference between the adversary’s advantage over synthetic and original data, where a high privacy gain can protect all records from membership and attribute inference attacks. In another study, Zhou et al. [117] use the absolute difference metric to estimate the privacy risk for property inference attacks. The metric is calculated between training samples’ inferred and ground truth proportions.

## 3.2 Generalization-based Metrics

Generalization refers to the model’s ability to learn and predict the pattern of unseen data drawn from the same distribution of training datasets. Recent studies measure privacy by the proportion of overfitting in generative models and diversity-based metrics.

### 3.2.1 Proportion of Overfitting

Overfitted models closely learn the training data and perform poorly on unseen data. If an overfitted model has a larger generalization gap, it makes this model vulnerable to membership inference. The generalization gap is the difference between model performance for training and hold-out data drawn from the same distributions. Chen et al. [21] measure the privacy of GANs by considering an extreme overfitting situation, which leads to a high generalization gap. The idea is to reduce the generalization gap to fix overfitting. This study uses multiple discriminators trained on disjoint partitions, where the generalization gap is measured by comparing the distribution of the discriminator’s prediction scores between training and holdout data. Besides, they use two distance-based metrics, namely Wasserstein distance and Jensen Shannon divergence, to measure the similarity between two probability distributions, where similar distributions represent a smaller generalization gap. Their findings suggest that increasing disjoint partitions provide a similar distribution between training and holdout samples. Overall, multiple discriminators improve the generator’s generalization ability, which can fix the overfitting problem.

### 3.2.2 Diversity-based metric

A valuable property of a generative model is to produce diverse samples. Liu et al.[68] investigate how the diversity of generative models can serve as evidence of generalization using a geometric diversity metric, dispersion. The generated and original data distribution dispersion scores in early training might be similar since the model may not generalize well. Later, when the model starts to generalize well, more diverse samples are produced, achieving a greater dispersion. However, Liu et al. [68] suggest that model generalization and diversity are inconsistent.

## 3.3 Differential Privacy-based Metrics

Differential privacy (DP) is a well-known approach that promises to protect individual training samples in generative models. A parameter epsilon ( $\epsilon$ ), known as privacy budget, controls the privacy level in DP. Many studies have adopted differential private training in generative models, where  $\epsilon$  quantifies privacy by noise-adding mechanisms. The most common approach is to train the model using DPSGD (Differentially Private Stochastic Gradient Descent), adding Gaussian noise to the gradients during training. Others involve the PATE (Private Aggregation of Teacher Ensembles) mechanism, which is training distributed teacher models to transfer knowledge to generators.

### 3.3.1 epsilon in DPSGD

Abadi et al. [1] introduced DPSGD for complex networks, ensuring a provable privacy guarantee in training samples. The DPSGD training procedure has two steps. First, gradients for model weights are computed from the loss of processed batch samples, and then computed gradients are clipped to control their sensitivity. The second step involves adding Gaussian noise to clipped gradients, updating the model, and estimating cumulative privacy loss with Moment Accountant. Finally, the training procedure terminates when the privacy budget is exhausted. Since its introduction, many researchers have used DPSGD to train GANs and VAEs using different noise-adding mechanisms, indicating effective use of privacy budget. Additionally, some studies work to improve convergence in learning algorithms by



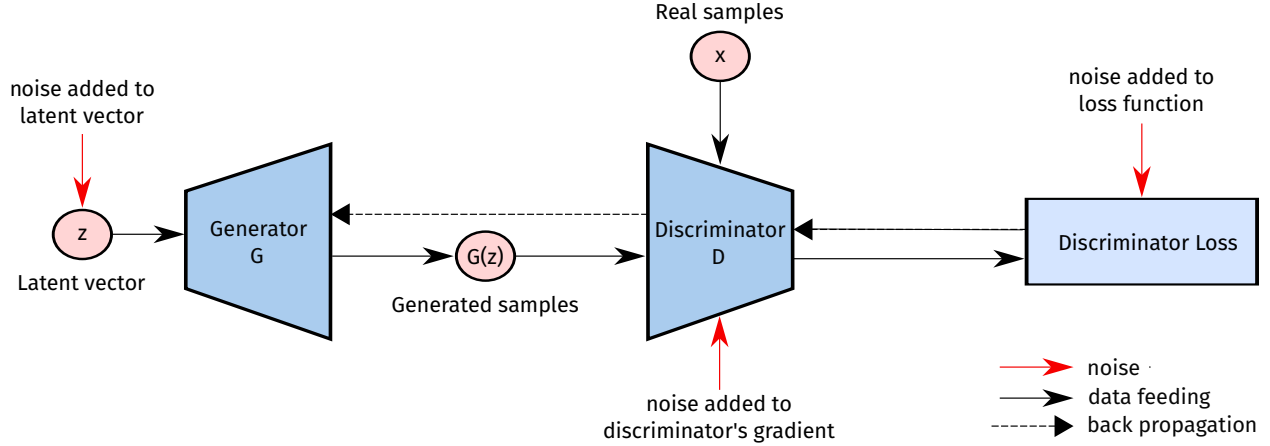


Figure 3: Noise Addition strategies in GANs

improving optimization strategies, which helps reduce privacy budget consumption. Hence, we have classified the noise perturbation strategies into four categories: noise addition to the discriminator’s gradient in GANs, noise addition to the discriminator’s output or loss function in GANs, noise addition techniques in VAEs, and noise addition to the latent vector in generative models. The various noise addition techniques in GANs are highlighted in Figure 3.

**Noise addition to the discriminator’s gradient in GANs** This is the most common strategy, where noise is perturbed to the discriminator’s gradient. The idea is that the generator network trained by the differential private discriminator becomes differential private due to the post-processing property of DP. While choosing an appropriate privacy budget in DP remains unclear, researchers have shed light on how the sequence of noise addition affects privacy in practice. For example, carefully choosing the noise variance during training or using a strong composition theorem of DP for a tighter privacy budget. Yang et al. [110] have used dynamic noise allocation strategies during the discriminator’s training [110]. The idea is to add more noise during model training’s early stages and gradually reduce it as parameters approach the optimal point to minimize the impact on convergence. This approach is further used in another study with a concentrated DP composition [85]. The study employs two adaptive noise allocation schemes, uniform and exponential decay, to dynamically choose the noise variance for the gradient. Uniform noise reduction to the minimum, whereas exponential decay indicates the noise scale decays exponentially.

Xie et al. [105] propose a privacy-preserving mechanism using the WGAN objective [6] by adding noise to the gradient of Wasserstein distance during the discriminator’s training. This study uses a weight clipping strategy instead of gradient clipping like DPSGD, which helps the gradient automatically be bound by some constant to reduce privacy costs. However, Xu et al. [106] suggest that adding noise to Wasserstein distance gradients could lead to significant privacy loss due to slower convergence compared to regular GANs. They introduce an adaptive gradient pruning strategy to track gradient magnitudes and dynamically adjust the pruning based on gradient updates. Moreover, Alzantot et al. [5] use improved WGAN objectives [41] to compute the gradient loss based on critic parameters from training data and add noise to the sum of clipped per-sample gradient. Further, Frigerio et al. [33] propose clipping decay where the clipping bound decreases with each generator update.

Torkzadehmahani et al. [100] propose a privacy-preserving framework with CGAN objective [78] by clipping the gradients of discriminator loss on real and synthetic data separately. This study splits the discriminator’s loss between real and synthetic data and then clips and sums the gradients of the two losses. Therefore, better control of the model’s sensitivity can improve privacy. Also, they prefer the RDP mechanism over moment accounting, which offers a relaxed definition of DP that supports advanced composition theorems [77]. In another study, Chen et al. [16] use an RDP accountant to train a discriminator privately with the improved WGAN objective [41]. First, they adopt a subsampling strategy to reduce the privacy cost, where the whole dataset is subsampled into different subsets to train multiple discriminators. Second, they selectively apply a noise-adding mechanism instead of gradient clipping like DPSGD, which helps to choose an optimal clipping value for a necessary subset of gradients, reducing noise effectively. This approach is further used in a few studies [116, 62]. Besides, some researchers prefer Laplace noise to train the discriminator privately in GANs [52, 47].

**Noise addition to the discriminator’s output or loss function in GANs** Han et al. [43] describe that existing frameworks that add noise to the gradient of discriminator’s network during training are time-consuming and can decline

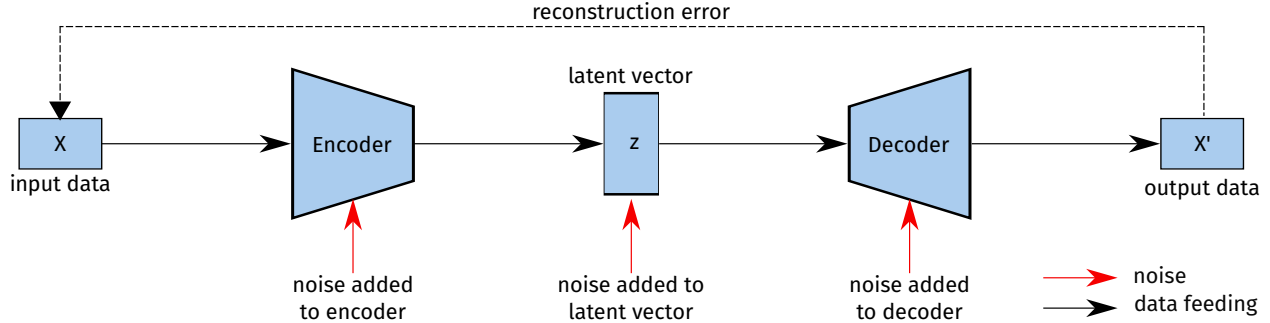


Figure 4: Noise Addition Strategies in VAEs

training performance. This study focuses on efficient differential private GANs by adding noise to the discriminator’s output or loss function. The idea is that by adding noise to the discriminator’s loss function, the generator becomes differentially private by the post-processing property of DP. They clip the discriminator’s loss first and then add Gaussian noise to it. Ma et al. [73] propose a framework, RDP-GAN, where the Gaussian noise is added to the loss function of the discriminator for each iteration. They use an adaptive noise tuning strategy that dynamically adjusts the noise scale during training, allowing less noise addition into loss functions.

**Noise addition techniques in VAEs** Researchers have used different noise-adding mechanisms for VAEs, described in Figure 4. Acs et al. [3] measure privacy using kernel-based clustering algorithms using a mixture of generative models, such as VAEs and RBMs (Restricted Boltzmann Machines). They describe that using mixture models requires less noise during training than single-model iterations. Also, this study partitions clusters and then trains the generative model on each cluster with DPSGD. Their findings suggest that using a mixture of generative models can require fewer training epochs than a single model, allowing less noise introduction. In another study, Jiang et al. [53] train the decoder privately using a subsampling strategy, where the dataset is randomly sampled and needs less noise than the full dataset. Moreover, some studies estimate privacy with the two-phase training procedures, using GANs and autoencoders [99, 97]. The idea is that when GANs are paired with autoencoders, the generator learns latent distributions accurately while the encoder reduces data dimensionality, allowing controlled noise injection. For instance, Torfi et al. [99] use CGAN [78] and convolutional autoencoder, using RDP accountant for tighter privacy analysis while noise is added to the clipped gradient of the encoder and decoder.

**Noise addition to the latent vector in generative models** Some papers use private latent vectors to train generative models [19, 96]. The intuition is that adding noise to the latent vector may reduce the privacy cost compared to injecting noise during model training. For instance, Chen et al. [19] design a differential private model inversion strategy to improve privacy over DPSGD-based GANs in two scenarios. First, a higher-dimensional GAN is trained with public data in the public domain, where no noise is introduced. Second, the resulting GAN is placed in the private domain, where a model inversion attack is performed to retrieve the latent vector. Then, a lower-dimensional GAN is trained with the collected latent vectors. Overall, privacy costs are reduced since no noise is introduced in the private domain, and the lower-dimensional GANs deal with less complex structures. In another study, Takagi et al. [96] use an encoder-decoder network in a two-phase training procedure. First, the latent vector is privately trained with the DP-EM (Differentially Private Expectation Maximization) algorithm at the encoding phase. Then, the encoder is trained following the distributions of the latent variables. Second, at the decoding phase, the decoder is trained with the encoder, which improves training stability and increases noise resistance.

### 3.3.2 epsilon in PATE

PATE is a generic approach providing DP guarantee in training samples, introduced by Papernot et al. [86]. In this method, the original sensitive dataset is partitioned into disjoint subsets, and then a teacher model is trained on each subset. The teacher model trains a student model while protecting the privacy of individual datasets. The main advantage is independent teacher training without restriction, where the predictions of all teachers’ models are aggregated with noise-adding mechanisms to achieve the DP guarantee. Ultimately, knowledge transfer from the teacher models achieves a privacy-preserving student model. Inspired by this approach, some researchers have used PATE to train GANs privately. The noise addition technique through PATE mechanisms against GANs is described in Figure 5.

**Noise addition techniques in PATE-GANs** Jordon et al. [55] propose a framework, namely PATE-GAN, to train the GANs privately for multi-variate tabular data. The idea is to train distributed discriminators to transfer knowledge to the

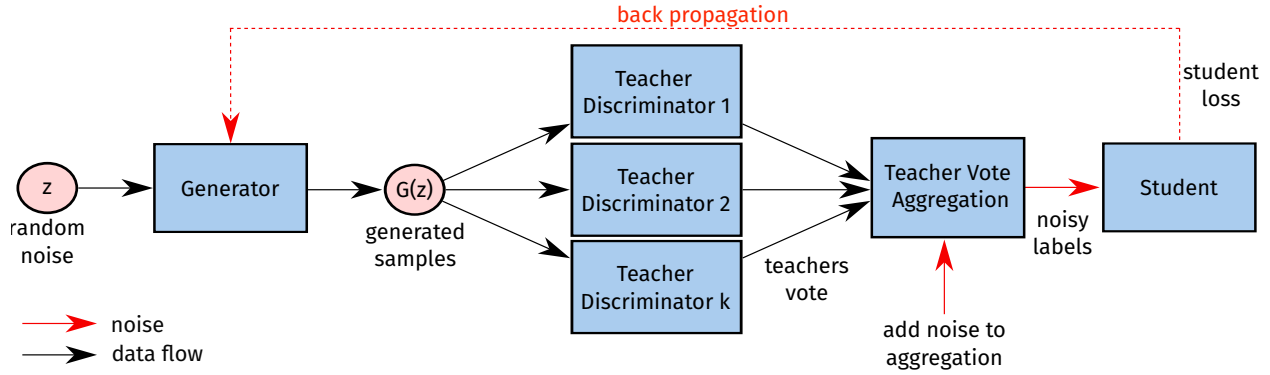


Figure 5: Noise Addition Techniques in GANs by PATE Mechanism [55]

generator without an auxiliary public dataset. The teacher discriminators are trained individually on disjoint partitions of the training dataset, accessing only partial data. Then, the student discriminator is trained with generated samples labeled by the teachers using the PATE method. Accordingly, the generator is trained to minimize its loss function concerning the student discriminator. Consequently, the student model can be trained privately without public data, allowing the generator to improve sample quality.

In another study, Long et al. [70] use a private gradient aggregation strategy that adds noise to the information flows from the teacher discriminators to the student generator. Additionally, the aggregation mechanism includes gradient discretization and random projection to reduce the privacy budget used by each aggregation step. Random projection also reduces the dimensionality of gradient vectors on which the aggregation is performed. Furthermore, Zhuo et al. [118] introduce a knowledge transfer framework, namely differentially private knowledge distillations that combine with GANs to transfer knowledge from teacher to student network. This study uses a privacy amplification strategy while adding noise to the sampled batch of distilled knowledge. Privacy amplification ensures that subsampling techniques are used efficiently for the privacy budget.

## 4 Utility Metrics in Generative Models

In generative models, utility metrics measure and compare the efficacy of synthetic data. The intention is that synthetic data can complement or replace real data for training/inference purposes. High-quality synthetic data can be used for useful cases, while low quality generated data can lead to biases and inaccuracies. There are a variety of utility metrics depending on a wide range of applications. For instance, some users may be interested in finding the similarity between real and synthetic samples, while others pay attention to inferring information from the population during specific tasks. Based on this perspective, we propose a taxonomy of utility metrics, categorized into two parts: specific utility-based metrics and fidelity-based metrics, highlighted in Figure 6.

### 4.1 Specific Utility-based Metrics

These metrics measure the utility of synthetic data for particular analysis by comparing the results with real data, such as classification or regression tasks. Classification-based metrics measure the classifier’s performance, whereas regression-based approaches assess the performance of predictive modeling. On the other hand, clustering-based metrics groups the data points into clusters based on their similarities or patterns.

#### 4.1.1 Classification-based Metrics

These metrics measure how well synthetic data can complement real data in downstream classification tasks. The intuition is to assess the quality of synthetic data trained on machine learning models using different classifiers and test them on holdout data. Researchers have used various classification-based metrics derived from the confusion matrix, such as accuracy, precision, recall, or F1-score, to measure the performance of synthetic data. Some studies also use other classification-based metrics, such as AUROC or AUPRC, to evaluate the classifier’s performance.

**Accuracy** This metric represents how well the generative model has learned the underlying distributions within the data, correctly predicting the class labels of their respective classes. Xu et al. [107] use random samples from synthetic data to perform classification tasks against GANs, where the utility of generative models improves with the increased

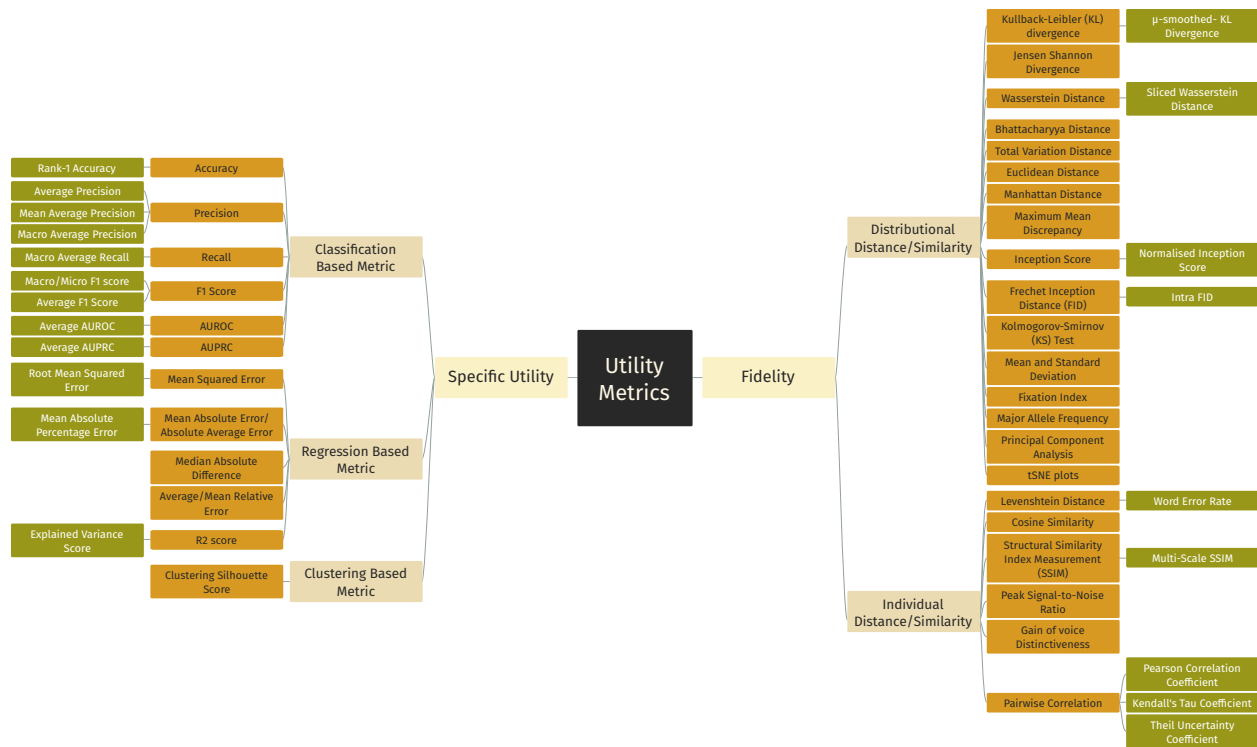


Figure 6: Taxonomy of Utility Metrics in Generative Models

training samples. Regarding image-based datasets, researchers have measured the classification accuracy using different classifiers to distinguish whether the input images with a predefined label belong to the correct label [73, 43, 16]. Ganey et al. [35] show that accuracy works better with balanced datasets than with imbalanced ones. Additionally, Frigerio et al. [33] empirically show that achieving high accuracy depends on the strong correlations between different features. In another study, Zhuo et al. [118] use Rank-1 accuracy, which refers to the percentage of predictions where the top prediction matches the ground-truth label to determine whether the ground-truth label equals the predicted class label with the highest probability.

**Precision/Recall** Researchers have used these metrics for binary and multi-class classification problems. For instance, Ganey et al. [36] use precision and recall in binary and imbalanced multi-class classification problems with two classes: minority and majority classes/subgroups. Because precision quantifies the number of correct positive predictions made, it calculates the accuracy for the minority class. In another study, Kunar et al. [62] use the Average Precision score, which uses a set of classifiers, whereas precision represents a specific classifier in a binary classification problem. Additionally, Zhuo et al. [118] use the Mean Average Precision, which is the average of the Average Precision of each class. Moreover, some researchers have used Macro Average Precision, estimated by averaging the precision values calculated for each class without considering the class imbalance [60, 19]. These papers also use Macro Average Recall to show the model performance across all classes rather than focusing on classes with more samples. This is calculated as the sum of recall scores for all classes divided by the number of classes.

**F1-Score** Researchers have used this metric to show how synthetic data works on classification tasks for imbalanced classification problems against generative models [97, 91, 60, 62, 116]. Xu et al. [108] use the Average F1-score, which is the weighted average of the class-wise F1 scores, where the number of samples available in that class determines the weights. Some studies use Micro and Macro F1-score for multi-class classification problems against GANs [19, 63, 108, 58]. The intuition is to calculate an overall F1 score for a dataset with more than one class. The Macro F1 score calculates the F1 score for each class and then averages them. In contrast, the Micro F1 score calculates the total of True Positives (TP), False Positives (FP), and False Negatives (FN) for all classes and then calculates the F1 score from these totals. The Micro F1 score is useful for overall performance, whereas the Macro F1 score ensures all the classes perform well for imbalanced datasets.

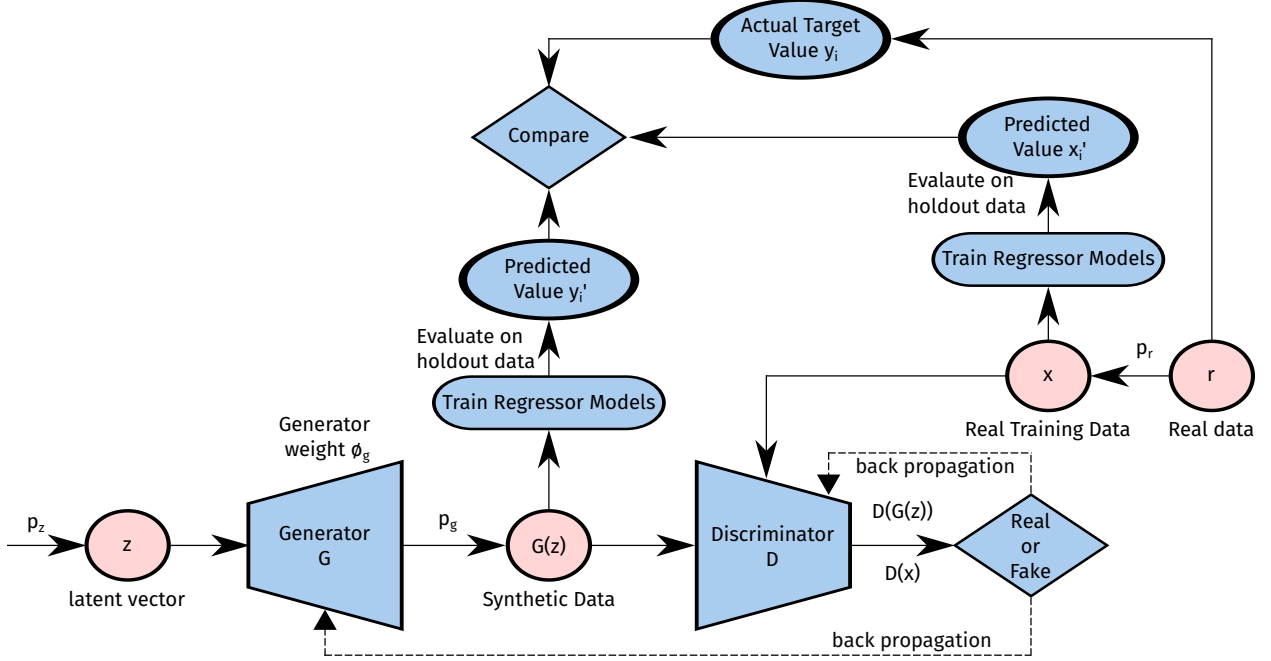


Figure 7: Evaluation Workflow of GAN-based Synthetic Data on Regression Tasks

**AUROC** Researchers have used this metric in binary classification tasks to assess classifier performance on synthetic data, comparing how well the model distinguishes positive and negative classes with real data [105, 70, 96, 111]. Jordon et al. [55] use the Average AUROC score to show how well synthetic data captures the characteristics of real data against PATE-GANs for multiple models.

**AUPRC** Torfi et al. [99] suggest that AUPRC is more useful than AUROC for imbalanced classification problems. This is because AUPRC focuses on precision-recall trade-offs, particularly on finding the minority/rare true positive classes, which is crucial in imbalanced data. In another study, Jordon et al. [55] use an average AUPRC score across all classes, providing an overall performance measure for multi-class classification problems.

#### 4.1.2 Regression-based Metrics

The idea for calculating this metric is that the synthetic and real training data are trained on regression models and tested on hold-out data. An evaluation workflow on GAN-based synthetic data in regression analysis is shown in Figure 7, where the actual target value of real data, i.e.,  $y_i$ , is compared with the predicted values of synthetic data, i.e.,  $y_i'$  and real training data, i.e.,  $x_i'$ . These metrics predict a value by calculating an error score to show the model's predictive performance, such as mean squared error, mean absolute error, median absolute difference, or mean/average relative error. Besides, statistical regression-based metrics, i.e., R-squared ( $R^2$ ) score, show the predictive performance of synthetic data compared to real data. The definition of all notations in regression tasks is shown in Table 1.

**Mean Squared Error (MSE)/Root Mean Squared Error (RMSE)** The MSE of synthetic data is derived as the average of squared differences between actual target values produced by real data and predicted values generated by synthetic data. Similarly, Root Mean Squared Error (RMSE) is an extension of MSE, which calculates the squared root of MSE. RMSE is preferred over MSE because it provides results in the same units as the target variable, making it easier to understand the significance of errors. The MSE of synthetic data are defined in Equation 1, where all the notations are described in Table 1:

$$MSE = \frac{1}{n} \sum_{i=1}^n (y_i - y_i')^2 \quad (1)$$

Lee et al. [63] use MSE to demonstrate the quality of synthetic data for downstream regression tasks against GAN using tabular data. In another study, Ho et al. [47] use RMSE to show the utility preservation of synthetic data using time-series datasets against GANs while applying this metric at each sampling time slot.

Table 1: Notation

Notation	Definition
$G$	Generator Network
$\phi_g$	Generator weight
$D$	Discriminator Network
$z$	Latent vector
$p_z$	Distribution of latent vector
$r$	Real data
$x$	Real training data
$p_r$	Distributions of real training data
$G(z)$	Synthetic data
$p_g$	Distribution of synthetic data
$y_i$	Actual target value of the $i$ -th record of real data
$y_i'$	Predicted value of the $i$ -th record of synthetic data
$x_i'$	Predicted value of the $i$ -th record of real training data
$n$	Number of samples in the test dataset

**Mean Absolute Error (MAE)/Mean Absolute Percentage Error (MAPE)** The MAE, also known as Absolute Average Error (AAE), of synthetic data, is estimated as the average of the absolute error values between actual target values on real data and predicted values on synthetic data. The MAPE of synthetic data measures the average absolute percentage error between the actual target values on real data and predicted values on synthetic data. MAPE is a scale-independent metric that can exceed 100%, allowing for better comparison of results across datasets with different units. The Equation 2 represents the MAE of synthetic data:

$$MAE = \frac{1}{n} \sum_{i=1}^n |y_i - y_i'| \quad (2)$$

Some studies use these metrics against GANs where the synthetic data is trained using different regression models and tested on hold-out data to compare the predicted values with actual target values [116, 63, 73].

**Median Absolute Difference (MAD)** This metric is calculated considering the median absolute differences between each data point and the overall median while comparing actual target values with predicted values. MAD of synthetic data is expressed in Equation 3, where  $\bar{y}_i = \text{median}(y_i)$ :

$$MAD = \text{median}(|y_i - \bar{y}_i|) \quad (3)$$

Webster et al. [102] consider MAD to show how well the synthetic data captures the real data’s features in vision tasks.

**Mean Relative Error (MRE)** This metric measures the average errors, which are expressed as percentages. It focuses on the relative rather than absolute difference between actual and predicted values. This metric is also called Average Relative Error (ARE), shown in Equation 4:

$$MRE = \frac{1}{n} \sum_{i=0}^{n-1} \frac{y_i - y_i'}{y_i} \times 100\% \quad (4)$$

AcS et al. [3] use ARE to show the performance of synthetic data in regression tasks for time-series datasets. Besides, Gursoy et al. [42] use ARE for privacy-preserving location trace problems while comparing actual and predicted answers for spatial counting queries.

**R-Squared ( $R^2$ ) Score** This metric represents a dependent variable’s variance ratio, which is further explained by an independent variable. In other words, the  $R^2$  score assesses how well a regression model explains the variance in the data on which synthetic data is trained. This is also called Explained Variance, where a value of 0 shows a poor fit, and 1 indicates a perfect fit. The Equation 5 represents the  $R^2$  score for a linear regression model:

$$R^2 = \frac{SS_{regression}}{SS_{total}} \quad (5)$$

In equation 5,  $SS_{regression}$  represents the variance explained by the model, which measures how well the regression model describes the data used for modeling.  $SS_{total}$  shows the total variance, which measures the variation in the

observed data. The total variance is measured by the sum of squares of the difference between predicted values and the actual target, described in Equation 6:

$$SS_{total} = \frac{1}{n} \sum_{i=1}^n (y_i - \hat{y}_i)^2 \quad (6)$$

Tantipongpipat et al. [97] report  $R^2$ -score using Lasso regression algorithms to measure the performance of synthetic data in regression analysis using mixed-type tabular data. Their empirical findings show that the synthetic data with continuous features has a negative  $R^2$ -score due to the lasso regression penalty term.

### 4.1.3 Clustering-based Metrics

These metrics measure the similarities between data based on their characteristics, grouping similar data objects into clusters while evaluating cluster distinctness using distance functions. The distance function differs with variables such as boolean, categorical, ratio/ordinal, and interval-scaled, where weight is associated with the variables based on their applications. Some researchers have adopted clustering-based metrics to measure the quality and performance of synthetic samples compared to real ones in clustering algorithms, e.g., clustering silhouette score.

**Clustering Silhouette Score (CSS)** This metric compares how close each cluster point is to the neighboring cluster’s points. The range of CSS is  $-1$  to  $1$ , where a higher score indicates the clusters are distinct. CSS is described in Equation 7:

$$CSS = \frac{a - b}{\max(b, a)} \quad (7)$$

In Equation 7,  $b$  shows the average distance between each point of a cluster, whereas  $a$  indicates the average distance between all clusters. Kim et al. [58] use CSS to evaluate the quality of generated samples using GANs for tabular datasets. They use the  $k$ -means clustering algorithm to group the data in real and generated samples and then calculate the silhouette score based on the resulting clusters.

## 4.2 Fidelity-based Metrics

Fidelity measures how well the synthetic data in generative models matches the real data. This metric measures the quality of synthetic samples, where high fidelity shows their close distribution with real data. There are two common approaches to fidelity-based metrics: distributional or population level and individual sample level. The distributional or population-level fidelity metrics focus on the overall distributions of data points, i.e., how frequently each value appears in synthetic and real data distributions. Different ways, such as probability distributions, statistical tests, or histogram/visual representations, can compare overall distributions between real and synthetic data. In contrast, the individual sample-level metrics compare the individual data points, calculating the distance or similarity between specific synthetic and real data values. Many researchers have measured the quality of synthetic samples using different datasets, such as images, tabular data, time series, graphs, audio/video, and genomics.

### 4.2.1 Distributional Distance/Similarity-based Metrics

These metrics measure the difference between the entire distributions of real and synthetic data, focusing on the overall features or characteristics of the distributions rather than individual data points. Researchers have calculated the distributional distance or similarity by comparing probability distributions between synthetic and real data, such as Kullback-Leibler (KL) Divergence, Jensen-Shannon Divergence (JSD), Wasserstein Distance (WD), Bhattacharyya Distance (BD), Total Variation Distance (TVD), Euclidean Distance (ED), Manhattan Distance (MD), Maximum Mean Discrepancy (MMD), Frechet Inception Distance (FID) or Inception Score (IS). Besides, some papers have explored statistical similarity-based metrics, such as Mean and Standard deviation, Kolmogorov-Smirnov (KS) Test, Fixation Index (FI), or Major Allele Frequency (MAF), and visual representation-based metrics, such as Principal Component Analysis (PCA) or t-distributed Stochastic Neighbor Embedding (tSNE) plots, to compare real and synthetic data.

**Kullback-Leibler (KL) Divergence** The KL divergence between two discrete probability distributions, such as  $p_r$  for real data and  $p_g$  for synthetic data, is defined in Equation 8:

$$D_{KL}(p_r || p_g) = \sum_{x \sim X} p_r(x) * \log \left( \frac{p_r(x)}{p_g(x)} \right) \quad (8)$$

where  $X$  is a random variable for all possible values to  $x$ . Additionally,  $p_r(x)$  and  $p_g(x)$  represent the probability of value  $x$  occurring for the real and synthetic data distributions. Goncalves et al. [39] use KL-divergence to compare

real and synthetic data distributions using tabular datasets, focusing on marginal probability mass functions (PMFs) for specific variables rather than entire datasets. In another study, Tantipongpipat et al. [97] have explored a variant of KL-divergence, i.e.,  $\mu$ -smoothed KL-divergence between the real and synthetic distributions. This metric is used because standard KL-divergence struggles with zero probabilities in one distribution while  $\mu$ -smoothed KL-divergence offers a solution, represented in Equation 9:

$$D_{\mu}(p_r||p_g) = \sum_{x \sim X} (p_r(x) + \mu) * \log\left(\frac{p_r(x) + \mu}{p_g(x) + \mu}\right) \quad (9)$$

For example, in some cases where  $p_r(x)$  is zero in Equation 8, while  $p_g(x) > 0$ , KL-divergence becomes undefined.

**Jensen-Shannon Divergence (JSD)** The JSD between two probability distributions is expressed in Equation 10, where  $M$  is the mixture between real and synthetic data distributions.  $D(p_r||M)$  and  $D(p_g||M)$  represent the KL Divergence from the real and synthetic data distribution to the mixture distribution:

$$JSD(p_r||p_g) = \frac{1}{2} * [D(p_r||M) + D(p_g||M)] \quad (10)$$

Kunar et al. [62] use this metric to measure the difference between the probability mass distributions of categorical variables in the real and synthetic data. However, their empirical findings suggest that the JSD is unsuitable for continuous variables while real and synthetic data overlap. Moreover, Zhao et al. [116] report that this metric is symmetric, which helps to interpret the experimental results easily by treating real and synthetic distributions equally. In another study, Gursoy et al. [42] use this metric using location trace datasets to compute trip distributions of real and synthetic data, where JSD quantifies the trip error.

**Wasserstein Distance (WD)** This metric, known as Earth Mover Distance (EMD) or Wasserstein-1 Distance, measures the work needed to transform one distribution (synthetic data) to another (real data) by moving data points or mass. This metric considers the absolute distance difference, where a lower distance shows similarity. Equation 11 defines the Wasserstein Distance between two probability distributions, such as real and synthetic data distribution in a metric space  $X$ , denoted as  $W_q(p_r, p_g)$ , where  $q$  is the exponent on the distance function used to calculate the cost of transporting mass between two probability distributions:

$$W_q(p_r, p_g) = \left( \inf_{\gamma \in \Gamma(p_r, p_g)} \int_{X \times X} d(x, y)^q d\gamma(x, y) \right)^{\frac{1}{q}} \quad (11)$$

where 11,  $\Gamma(p_r, p_g)$  represents the set of all joint probability distributions, i.e.,  $\gamma$  on  $X \times X$  whose marginals are  $p_r$  and  $p_g$ . Additionally,  $d(x, y)$  shows the distance between two points, such as  $x$  and  $y$  in the metric space  $X$ . Some studies have explored WD for continuous variables because min-max normalization, a key pre-processing step of WD, mitigates scale dependency issues when comparing distributions across features with varying scales, which is useful for continuous variables [62, 116]. In another study, Karras et al. [56] use sliced Wasserstein distance, an alternative WD, to compare the probability distributions in high-dimensional settings. Because WD is computationally expensive for high-dimensional complex data, sliced Wasserstein distance overcomes this situation by approximating the high-dimensional distributions into multiple one-dimensional slices, calculating WD for each, and then the obtained distances are averaged.

**Bhattacharyya Distance (BD)** This metric quantifies the similarity of two random distributions involving a Bhattacharyya coefficient. BD limits from 0 to 1, where a higher BD indicates the dissimilarity of two distributions. The BD for the two statistical distributions is expressed in Equation 12:

$$D_B(p_r, p_g) = -\ln(BC(p_r, p_g)) \quad (12)$$

where

$$BC(p_r, p_g) = \sum_{x \sim X} \sqrt{p_r(x)p_g(x)} \quad (13)$$

In Equation 13,  $BC(p_r, p_g)$  is the Bhattacharyya coefficient for discrete probability distributions, and  $p_r(x)$  and  $p_g(x)$  are the probabilities of event  $x$  in two distributions. Bhattacharyya Distance translates the coefficient into a distance metric in Equation 12. Lu et al. [71] apply this distance metric to compare real and synthetic data distributions using tabular datasets, where a larger Bhattacharyya distance indicates the dissimilarity between two distributions.



**Total Variation Distance (TVD)** This metric, sometimes called variational distance, compares the similarity of two probability distributions. TVD is expressed in Equation 14, where the two probability distributions of real and synthetic data, such as  $a_r$  and  $a_g$  are defined in a sample space  $X$ , and  $B$  is the subset of the sample space, representing a specific event:

$$TVD(a_r, a_g) = \max_{B \subseteq X} |a_r(B) - a_g(B)| \quad (14)$$

In Equation 14,  $a_r(B)$  and  $a_g(B)$  represent the probabilities assigned to the subset  $B$  by the two distributions. Thus, TVD is estimated as the maximum absolute difference over all possible subsets  $B$  of  $X$ . Generally, this metric ranges from 0 to 1, where 0 signifies perfect similarity and 1 indicates maximum dissimilarity between two distributions. Takagi et al. [96] calculate the average of TVD of all 2-way marginals, i.e., relationships between pairs of variables of real and synthetic data. The intuition is that focusing on 2-way marginals helps identify the data's dependencies and capture the core relationship while handling the complexity of high-dimensional data. Moreover, they consider the average TVD because it helps reduce sensitivity to outliers by considering all possible shifts of one distribution relative to the other.

**Euclidean Distance (ED)** This metric measures the direct or straight line distance between two points in Euclidean space, where the data points can be represented as feature vectors. Accordingly, when ED is applied to vectors, it calculates the overall difference between the corresponding elements of two vectors. Equation 15 describes the Euclidean distance for two vectors, such as  $X$  and  $Y$ , of real and synthetic data, and  $n$  is the dimension of the feature vectors:

$$ED(X, Y) = \sqrt{\sum_{i=1}^n (x_i - y_i)^2} \quad (15)$$

Xu et al. [107] have used this metric to evaluate the closeness between synthetic and real datasets by considering the joint and conditional probabilities. They measure the Euclidean distance between the estimated probability vectors, namely probability mass function, derived from the sample space from the real and synthetic datasets. In another study, Hyeong et al. [51] use the average ED (column-wise), focusing on the similarity of individual features between real and synthetic datasets.

**Manhattan Distance (MD)** This metric, also known as  $L1$  distance, calculates the distance between two points. MD considers the sum of horizontal and vertical distances between two data points by comparing the absolute differences in individual features of real and synthetic data. Equation 16 defines the Manhattan Distance for two points  $x$  and  $y$ , regarding real and synthetic data, where  $n$  is the dimension of the feature vectors:

$$MD(X, Y) = \sum_{i=1}^n |x_i - y_i| \quad (16)$$

Although this metric focuses on how much individual feature value differs between a real and synthetic data point, applying it to an entire distribution makes it a distributional distance/similarity measure. For instance, Lu et al. [71] consider this metric to compare the entire distribution of node degrees between the real and synthetic data using social network-based graph datasets. They apply this metric to compare the node attributes, where each node is associated with attribute vectors representing some characteristics. In another study, Li et al. [66] have used  $L1$  distance to compare the occurrences of various activity types in real and synthetic process data, considering the overall distribution of activity frequencies.

**Maximum Mean Discrepancy (MMD)** This metric is a kernel-based statistical test that compares two probability distributions. It transforms the original data points into higher-dimensional feature spaces using kernel functions rather than comparing the original data points. MMD estimates the maximum difference between the average values of these transformed features across the two distributions, presented in Equation 17:

$$MMD(P, Q) = \|E_x \sim P[\phi(x)] - E_y \sim Q[\phi(y)]\|_{H^2} \quad (17)$$

where  $E_x \sim P[\phi(x)]$  and  $E_y \sim Q[\phi(y)]$  are the expected value of the transformed data point  $\phi(x)$  and  $\phi(y)$  under distribution  $P$  and  $Q$ .  $H^2$  is the squared norm in the Hilbert space  $H$ . Torfi et al. [99] use MMD to compare synthetic data to real data in a GAN framework because it is ideal for unsupervised settings and requires no labeled data. Also, it can effectively compare the distributions based on the inherent features captured by the kernel function.

**Cosine Similarity** This metric estimates the similarity of two vectors in multi-dimensional space by deriving the cosine angle between the real and synthetic data vectors. Equation 18 expresses the cosine similarity, where  $A$  and  $B$  represent the vectors of real and synthetic data points, and  $\theta$  is the angle between vectors  $A$  and  $B$ . Additionally,  $\|A\|$  and  $\|B\|$  are the magnitude of vector  $A$  and  $B$ :

$$\cos(\theta) = \frac{A \cdot B}{\|A\|\|B\|} \quad (18)$$

Sasada et al. [91] use this metric to compare the similarity between real and synthetic text. The idea is to focus on the directional similarity between two vectors using word frequencies in text, where high cosine similarity suggests similar overall distributions of words. In another study, Chen et al. [18] have used this metric to assess synthetic sequences against real ones in financial applications. They use this metric because it focuses on directional relationships between vectors rather than absolute positions or scales, which is ideal for time-series datasets.

**Frechet Inception Distance (FID)** Heusel et al. [45] first introduced FID to compare the distance between feature vectors calculated for real and synthetic images. This metric uses a pre-trained model, i.e., Inception  $v3$ , to retrieve the feature vectors for real and synthetic images. Then, the retrieved feature vectors are considered as datasets in a high-dimensional space. FID estimates the distance between these two feature vector distributions' statistical properties, such as mean and covariance. Equation 19 describes the FID score considering real and synthetic image distributions:

$$d^2 = \|\mu_\varphi(p_r) - \mu_\varphi(p_g)\|^2 + Tr \left( \Sigma_\varphi(p_r) + \Sigma_\varphi(p_g) - 2\sqrt{\Sigma_\varphi(p_r)\Sigma_\varphi(p_g)} \right) \quad (19)$$

where  $\mu_\varphi(p_r)$  and  $\mu_\varphi(p_g)$  are the mean of the feature vectors.  $\Sigma_\varphi(p_r)$  and  $\Sigma_\varphi(p_g)$  are the covariance matrices of the feature vectors for real and synthetic images.  $d^2$  distance in squared units between two feature vector distributions, and  $Tr$  is a trace operator estimated by summing the diagonal elements of the matrix. Long et al. [70] use this evaluation metric to show how well synthetic images capture the statistical properties of real images, where a lower FID corresponds to better quality synthetic samples with more similar distributions with real data. Miyato et al. [79] proposed an intra-FID score, which addresses the limitation of standard FID for conditional GANs [78]. The intra-FID computes individual FID scores for each condition the cGAN is trained on and then calculates multiple FIDs corresponding to each conditional setting. Moreover, Karras et al. [57] use the FID score to measure the quality of GAN-generated samples, where the FID score decreases while the training progresses. However, the FID score is reported as better early in training in another study [13].

**Inception Score (IS)** This metric measures the quality of synthetic images to show how realistic they are compared to real images. Salimans et al. [90] first proposed this metric for GANs, where a higher inception score indicates better-quality images. The inception score is calculated using a pre-trained image classification model, i.e., Inception  $v3$  model, to predict the class probabilities, i.e., conditional class labels for synthetic images. Equation 20 defines IS of a generator  $G$ , where  $z$  is the latent vector and  $G(z)$  is the synthetic image:

$$IS(G) = exp(E_{x \sim G(z)}[KL(p(y|x)||p(y))]) \quad (20)$$

In Equation 20,  $p(y|x)$  is the conditional class distribution for a given input image  $x$ , calculated by the inception- $v3$  model, and  $p(y)$  is the marginal class distributions of synthetic images. Additionally,  $KL(p(y|x)||p(y))$  is the KL-divergence of  $p(y|x)$  and  $p(y)$  and  $E_x$  is the expectation of synthetic images. Chen et al. [18] use this metric to evaluate the quality of GAN-generated images, where a larger IS score shows more diverse and better-quality synthetic images. In another study, Liu et al. [69] use a generated score, calculated by the mean of inception score, to evaluate the quality of generated images with real images.

**Mean and Standard Deviation** These metrics compare all data points between real and synthetic data. The mean represents the data distribution's central tendency. The standard deviation estimates the variation of the values in a dataset relative to the mean, described in Equation 21 and 22:

$$Mean = \sum_{i=1}^n \frac{x_i}{n} \quad (21)$$

$$SD = \sqrt{\frac{\sum(x_i - x_{bar})^2}{n - 1}} \quad (22)$$

In (21) and (22),  $x_i$  is the  $i$ -th sample in a dataset,  $n$  is the total number of samples, and  $x_{bar}$  is the mean of the sample. Li et al. [66] use these statistical measures to compare the distance between synthetic and real sequences, where the number of activities in process data represents sequence length.

**Kolmogorov-Smirnov (KS) Test** This non-parametric statistical test compares the probability distributions of two datasets, i.e., real and synthetic data. Because this non-parametric test does not require knowledge of the underlying distributions, it is suitable for real-world data. The *KS* test compares the two datasets’ empirical cumulative distribution functions (ECDF), indicating the probability that a proportion of observations is less than or equal to a certain value. The idea is that the *KS* test calculates a statistic, i.e.,  $D$ , by comparing the ECDFs, representing the maximum absolute difference between two distributions, where a higher value shows a larger difference between two distributions. Equation 23 defines the *KS* test statistic  $D$ , where  $F_P(x)$  and  $F_Q(y)$  are the *ECDF* of real and synthetic datasets at sample  $x$  and  $y$ . Additionally,  $F_P(x)$  at a point  $x$  is calculated in Equation 24, where  $n$  is the total number of samples in real dataset  $P$ :

$$D = \max|F_P(x) - F_Q(y)| \quad (23)$$

$$F_P(x) = \frac{\text{Number of samples in } P \leq x}{n} \quad (24)$$

In the *KS* test, a statistical reference table, the *KS* table, provides critical  $D$  values for various sample sizes at a significance level. A higher calculated value of the *KS* test statistic  $D$  than the critical  $D$  value suggests a low  $p$  value, indicating a significant difference between the two datasets’ distributions. The  $p$  is calculated by the test statistic  $D$  and the sample sizes using statistical software (Python or *R*). Oprisanu et al. [84] use this non-parametric test for genomic datasets to compare the real and synthetic samples. In another study, Imtiaz et al. [52] use *KS* test on the samples taken from the real and synthetic distribution, where a higher  $p$ -value, indicates a higher probability that the samples come from the same distribution.

**Fixation Index (FI)** This population genetics measure shows how much genetic variation exists between subpopulations. The fixation index ranges from 0 to 1, where a value of 0 indicates no genetic difference between subpopulations, and a value of 1 suggests a complete genetic variance. The FI of synthetic data is defined as the ratio of variance among subpopulations to the total population variance, reflecting genetic differentiation. Oprisanu et al. [84] have adopted this population genetics measure to show how the groups of populations differ. In particular, they measure the variance in allele frequencies between populations to compare synthetic data with real data.

**Major Allele Frequency (MAF)** This metric quantifies how frequently a most common allele occurs within a given population. The MAF of real or synthetic data is calculated as the ratio of major allele counts to the total number of alleles, the count of major and minor alleles. Oprisanu et al. [84] have considered this population genetics metric to show how well synthetic data complements real data against generative models. Additionally, they demonstrate that the sample size impacts MAF, where a larger sample size provides a more precise estimation of allele frequencies in a population.

**Principal Component Analysis (PCA)** This metric is a linear dimensionality reduction technique used to compare the similarities in patterns or structures between real and synthetic data through visual representations. PCA is called a dimensional reduction technique. First, it identifies the most significant variance in data by focusing on the top principal components. Then, it reduces the dimensionality of the data while retaining most information. This metric follows three steps: standardization and covariance matrix, eigenvectors, and eigenvalues. First, a range of continuous initial variables is standardized, preventing features with larger scales from dominating the analysis and allowing PCA to identify the most significant directions of variance. Then, the covariance matrix is used to capture the correlations, i.e., linear relationships between features within data. Second, the eigenvectors and eigenvalues of the covariance matrix are derived to identify the principal components. Eigenvalues refer to the variance explained by each principal component, and eigenvectors show the directions of these principal components. Finally, a feature vector is constructed to determine the retained principal components.

Yale et al. [109] use PCA to show the resemblance between synthetic and real data, whereas in another study, Xu et al. [106] use an extension of PCA, i.e., 2-way PCA, to analyze mixed-type complex datasets. The 2-way PCA considers two-dimensional data, applying individually to each dimension. Their study reports that PCA provides promising results by producing detailed distributions in complex datasets.

**t-distributed stochastic neighbor embedding (t-SNE)** This metric is an unsupervised non-linear dimensionality reduction technique that transforms high-dimensional data into a low-dimensional space for analysis and visualization. tSNE is used to visualize complex datasets into two or three dimensions, measuring the similarities by analyzing the underlying relationships. This minimizes the divergence between the original higher and lower-dimensional probability distributions. Then, the optimized lower dimension allows the visualization of the clusters and sub-clusters of similar data points. Meyer et al. [75] have considered the tSNE measure to compare real and synthetic speech data, where they report that the t-SNE plots become similar with increasing training iterations. In another study, Tian et al. [98]

demonstrate a fairness protection performance in facial images, where they apply a tSNE measure to compare biased training data and privacy-preserving synthetic data distributions.

#### 4.2.2 Individual Distance/Similarity-based Metrics

These metrics measure how similar individual data points are between real and synthetic data. In other words, these metrics quantify the distance/similarity between a pair of data points to assess how well synthetic data captures the structure and relationship of real data. Researchers have adopted individual distance or similarity-based metrics, such as Levenshtein Distance, Structural Similarity Index Measure (SSIM), Peak Signal-to-Noise Ratio (PSNR), Gain of Voice Distinctiveness (GVD), or Pairwise Correlation Metrics.

**Levenshtein Distance/Word Error Rate** This metric, also referred to as edit distance, measures the similarities between two sequences or strings, where the minimum number of operations, such as insertion, deletions, or substitutions, is required to transform from one sequence or string to another. Levenshtein Distance can be considered an individual distance and a distributional distance measure based on specific context. For example, Li et al. [66] have considered this metric for sequential/time-series datasets, applying this metric to the sequence variance to show the dissimilarity between sequences within a dataset. The intuition is to capture the overall variability within a set of sequences by comparing the Levenshtein distances between all pairs of sequences within the dataset. In another study, Meyer et al. [75] use Word Error Rate (WER) derived from Levenshtein Distance to compare the sequence of words of generated samples against the original sequence of words while focusing on the discrepancies between corresponding words.

**Structural Similarity Index Measurement (SSIM)** This metric measures the similarity between real and synthetic images by evaluating an image’s quality regarding luminance, contrast, and structure. This metric is calculated between the corresponding windows in the real and synthetic images at each scale, comparing the local patterns of pixel intensities. SSIM ranges from  $-1$  to  $1$ , where a value of  $1$  indicates perfect resemblance. SSIM is defined in Equation 25, where  $a$  and  $b$  are the windows of real and synthetic images,  $\mu_a$  and  $\mu_b$  are the pixel sample mean,  $\sigma_a^2$  and  $\sigma_b^2$  are the variance and  $\sigma_{ab}$  is the covariance of  $a$  and  $b$ :

$$\text{SSIM}(a, b) = \frac{(2\mu_a\mu_b + x_1)(2\sigma_{ab} + y_2)}{(\mu_a^2 + \mu_b^2 + x_1)(\sigma_a^2 + \sigma_b^2 + y_2)} \quad (25)$$

where  $x_1$  and  $y_2$  are the constants added to stabilize the division when the mean and covariance are close to zero. Croft et al. [25] have adopted this metric to measure the similarity of a facial obfuscated image to its real images in GANs. They calculate the average SSIM by comparing all obfuscated image pairs with identity classification accuracy. Researchers have also explored MS-SSIM, multi-scale variants of SSIM, which calculates a weighted average across scales for a more detailed image similarity assessment. Karras et al. [56] use MS-SSIM in the training configurations of PPGANs while comparing synthetic images with real ones. They report that this metric is sensitive to high-frequency textures because PPGANs focus on broader structures over finer details, where this metric offers limited information.

**Peak Signal-to-Noise Ratio (PSNR)** This metric quantifies the quality of synthetic images compared to real images, computed as the ratio between the maximum possible power of a signal/image, e.g., the maximum possible value of the data type and the background noise that affects the signal/image. The noise’s power affects the data’s fidelity, expressed in decibels (dB). PSNR is described in Equation 26, where  $MAX$  is the maximum possible pixel values of real images and  $MSE$  is the mean squared error:

$$\text{PSNR} = 10 \times \log_{10} \left( \frac{\text{MSE}}{\text{MAX}^2} \right) \quad (26)$$

Wen et al. [103] have adopted this metric to measure the similarity of synthetic facial images with real images against GANs. They consider PSNR to show how well the intensity values of pixels in synthetic images correspond to those in real images, where a low PSNR suggests poor reconstruction quality.

**Gain of Voice Distinctiveness (GVD)** This metric measures how closely a synthetic signal, i.e., the voice produced by a system, resembles the real signal, i.e., the human voice. GVD measures how well a voice processing system preserves the ability to distinguish between different speakers. This metric can be computed using different approaches, consisting of voice similarity metrics that compare the acoustic features. GVD values can be positive or negative, where a positive value indicates that the distinctiveness is preserved between real and synthetic voices. Meyer et al. [75] have applied this metric to evaluate the fidelity in a speaker anonymization process, which aims to hide the identity of a speaker by changing the voice during speech recordings. They use GVD to measure the difference in voice characteristics to show how well synthetic voices produced by GANs from various speakers remain distinct compared to the real speaker’s voice.

**Pairwise Correlation Metrics** These metrics measure the linear relationship within real or synthetic data between all possible pairs of variables. In other words, it calculates the correlation for each pair of variables, resulting in a correlation matrix. Goncalves et al. [39] calculate pairwise correlation differences (PCD) to show how well the synthetic data captures the underlying correlation among the variables regarding real data. PCD is expressed in Equation 27, where  $A_r$  and  $A_s$  are the real and synthetic data matrices:

$$PCD(A_r, A_s) = \|\text{Corr}(A_r) - \text{Corr}(A_s)\|_F \quad (27)$$

In Equation 27,  $F$  is the Frobenius norm of the Pearson Correlation Matrices, calculated from real and synthetic datasets, where a smaller PCD suggests closer linear correlations across the variables. Chen et al. [19] have used the Pearson Correlation Coefficient (PCC) for time-series datasets that measure the linear relationship between two continuous variables. This metric ranges from  $-1$  to  $1$ , where  $1$  and  $-1$  signify a linear relationship, and  $0$  indicates no linear relationship. This metric is presented in Equation 28, where  $x_i$  and  $y_i$  are the individual data points regarding real or synthetic data,  $n$  is the number of data points, and  $\bar{x}$  and  $\bar{y}$  are the mean values of  $x$  and  $y$ :

$$PCC = \frac{\sum_{i=1}^n (x_i - \bar{x})(y_i - \bar{y})}{\sqrt{\sum_{i=1}^n (x_i - \bar{x})^2 \sum_{i=1}^n (y_i - \bar{y})^2}} \quad (28)$$

This metric is sensitive to outliers but performs well when the variables are normally distributed. In another study, Gursoy et al. [42] apply the Kendall-Tau Coefficient (KTC) metric to compare the ranks within individual pairs. This metric is a rank-based correlation coefficient without relying on assumptions about the underlying distribution, such as normal or uniform distributions. This metric ranks data points instead of actual values to compare variables, where all possible pairs of data points are compared based on their ranks. This metric is represented in Equation 29, where  $\tau$  represents Kendall Tau Coefficient ranging from  $-1$  to  $+1$ , and  $n$  is the total number of data points in a dataset:

$$\tau = \frac{\text{concordant pairs} - \text{discordant pairs}}{n \times (n - 1) / 2} \quad (29)$$

In Equation 29, concordant and discordant pairs indicate that the order of ranks of all pairs is the same and reversed regarding real or synthetic data. Moreover, Zhao et al. [116] use the Theil uncertainty coefficient (TUC) to measure the correlation between any two categorical features within real and synthetic datasets. Because they deal with tabular datasets, this metric is well-suited for comparing distributions of categorical variables. This metric is typically used in information theory, quantifying the degree of uncertainty reduction about one variable given the knowledge of another variable, ranges from  $0$  to  $1$  and is described in Equation 30 between two variables  $X$  and  $Y$ :

$$U(X|Y) = 1 - \frac{H(X|Y)}{H(X)} \quad (30)$$

In Equation 30,  $H(X|Y)$  is the conditional entropy of  $X$  given  $Y$ , measuring the uncertainty of  $X$  given the value of  $Y$  and  $H(X)$  is the unconditional entropy of  $X$ , measuring the uncertainty of  $X$  without considering  $Y$ . This metric works well to capture both linear and non-linear relationships.

## 5 Summary and Future Research Directions

This article comprehensively reviews publications on the latest developments in privacy-preserving generative models, focusing on privacy attacks and metrics for privacy and utility. Starting with approximately 1200 papers, we identified 100 research publications for in-depth analysis, facilitating different aspects of potential threats, privacy, and utility metrics on generative models. We provided an explicit overview of privacy and utility metrics in generative models in Section 3 and 4. Despite much progress in this field in recent years, several open challenges remain for improving the existing approaches. This section highlights three key questions about the open gaps that need to be solved in future research.

### 5.1 How to select privacy metrics in generative models considering the weaknesses and strengths in different metrics?

As demonstrated by several studies in Section 3, each category of metrics has distinct benefits and implications. We observed that attack-based classification metrics primarily focus on data or model-level privacy by measuring the adversarial success rate, and they do not offer formal guarantees about the level of model privacy protection. Although researchers have used different classification-based metrics, there is no silver bullet since the choice of each metric depends on the particular requirements of a problem. For instance, single-score metrics, e.g., accuracy, are most common due to their effectiveness for balanced datasets and holistic approach to understanding how the model performs

Table 2: Fidelity Metrics Based-on Data Types

Data Types	Utility Metrics	References
Image	IS, FID, PSNR, SSIM, KL-Divergence, JSD, WD	[81, 103, 61, 106, 102, 74, 8, 117, 70, 17, 25, 12, 56, 110]
Tabular	PCD, BD, JSD, TUC, KS Test, ED, WD	[71, 116, 52, 62, 39, 51, 97]
Time-Series	MMD, PCC, KTC	[42, 19, 10]
Audio/video	WER, GVD	[75]
Genomics	FI, MAF, KS Test	[84]

across all classes. However, for imbalanced and multi-class classification problems, AUROC or AUPRC is more appropriate. Additionally, accuracy fails to provide insight into the model’s prediction confidence and might overlook outliers. Similarly, outliers can influence precision metrics, potentially reducing True Positives. Besides, the recall fails to offer insights into the negative class instances.

Selecting privacy metrics that reflect both the average and worst case is often recommended [101]. However, distance/similarity-based attack metrics often focus on average-case performance and may not effectively address worst-case possibilities [37]. Even with a higher similarity, there could still be outliers in the data whose information remains vulnerable. Therefore, it may be beneficial to use robust distance-based metrics with less sensitive outliers, such as Median Absolute Deviation [64] or combining similarity/distance-based metrics with other methods, e.g., clustering with outlier detection [83].

A wide range of studies rely on differential privacy-based metrics, which ensures a measurable privacy guarantee. However, the implications of DP in generative models are wide-ranging. First, in DP, adding more noise improves privacy and reduces task accuracy [36, 62, 99]. Second, determining the right privacy budget is complicated, and researchers have investigated the optimal selection of privacy budget to protect their models [37]. This is likely due to the complexity of setting the epsilon value for unpredictable datasets, which have high sensitivity and make it harder to find an appropriate epsilon. Third, applying DP in healthcare can be challenging due to finite training samples [111]. DP works well with large datasets but may be less effective with limited samples, as added noise can distort underlying data patterns. Finally, DP has an unforeseen side effect of reducing accuracy in underrepresented subgroups [36]. While some researchers show DP has limited control over fairness [9], Cheng et al. [23] empirically explore that DP disproportionately increases the influence of majority subgroups, particularly in highly imbalanced datasets.

The generalization-based metrics improve model generalizability that can address overfitting problems to protect privacy in generative models [21]. Additionally, exploring the connection of the diversity of generative models with model generalization can be a promising research direction while measuring privacy [68]. Besides, some potential approaches, such as model pruning, knowledge distillation, and transfer learning, improve the model’s generalizability to enhance its performance on specific tasks [54, 114, 4]. Model pruning reduces unnecessary weights, resulting in a smaller and faster model. Likewise, the transferring knowledge strategy in knowledge distillation improves the model’s performance in adapting unseen data. Therefore, there is still scope for generalization-based metrics to improve privacy.

## 5.2 How to choose utility metrics for assessing generative models, considering their pros and cons?

As demonstrated by several studies in Section 4, the utility metrics are categorized into two parts. Section 5.1 already discusses several issues regarding classification-based metrics, which apply similarly to such metrics when used for utility. Besides, existing studies have used four categories of regression-based metrics: scale-dependent measures, such as MSE, RMSE, MAPE, and MAE; measures based on relative error, e.g., MRE; scaled error, e.g., MAD and goodness-of-fit metric, e.g., *R*-Squared score. However, there are no ideal metrics that satisfy all conditions. For instance, scale-dependent metrics, such as MSE or RMSE, are suitable when data is normally distributed; however, these are affected by outliers. For example, RMSE focuses on large errors, which might not be as important for capturing overall trends in time series data [7]. MAE and MAD, which consider absolute deviations, can better handle outliers in such cases. Moreover, MAPE, expressed as a percentage, makes comparing forecasts across time series with different scales challenging [31]. Also, its sensitivity to zero values can be problematic in time series datasets with frequent zeros or very low values. The *R*-Squared score works well for linear relationships; however, it is unsuitable for assessing predictive accuracy in numerical data, as it focuses on error direction rather than magnitude [65]. Therefore, researchers should consider suitable regression metrics depending on some specific context, such as the type of errors, outliers, or data distributions.

Regarding fidelity-based metrics, it remains unclear when their scores are meaningful and when they may be misinterpreted. For example, while PSNR measures image fidelity in preserving visual details [103], its relevance to audio fidelity for preserving sound quality is unclear. Similarly, pairwise correlation-based metrics are primarily applied for tabular and time-series datasets [116]; however, their efficacy for image datasets remains uncertain. This is likely because correlation-based metrics capture linear relationships, whereas image datasets often involve more complex relationships. Cosine similarity, used in text recognition [91], measures vector direction rather than magnitude, which could benefit other domains, i.e., time series analysis [104, 27]. Likewise, Maximum Mean Discrepancy (MMD), used for measuring distributional similarity for time-series datasets [99], can also be applied to other domains, such as tabular, image, or text due to its ability to capture complex relationships and flexibility of its kernel function [113, 14].

In some scenarios, the data types can impact the choice of fidelity-based utility metrics, described in Table 2. For instance, some standard metrics quantify the visual similarity of image datasets, such as IS, FID, SSIM, and PSNR. Researchers have used these because they provide quantitative measures, focusing on the perceptual similarity or human perception that assesses how well the synthetic images capture the underlying features of real images. However, human assessment tends to be biased toward the visual quality of generated samples, where evaluations can be inconsistent and hard to compare. Similarly, some metrics estimate different aspects of tabular datasets, such as numerical or categorical features, relationships, or distributions within data. For example, pairwise correlation considers linear relationships in numerical data, whereas Bhattacharyya Distance (BD) compares the probability distributions of categorical or binary features. Moreover, the Pearson Correlation Coefficient (PCC) is used in time series to estimate linear dependence, which makes it easy to interpret the trends. Maximum Mean Discrepancy (MMD) detects distributional differences, while the non-parametric Kendall-Tau Coefficient is robust to outliers, making it ideal for time-series analysis. Further, some metrics consider audio quality assessment, i.e., Gain of Voice Distinctiveness (GVD) or different aspects of genomic analysis, such as the Fixation Index (FD), Major Allele Frequency (MAF), or Kolmogorov-Smirnov (KS) test.

It is crucial to consider the target audience when choosing metrics. Simple metrics are easy to understand for non-experts, while visual comparisons are more attractive. Individual-based metrics provide limited scope, but merging them with distributional-based metrics can provide a detailed analysis. However, implementing them in a particular scenario can pose challenges due to specific metrics features that are not predicted, such as sensitivity to outliers, measurement bias, issues in data quality, or incompatibility in some contexts. Because there is no one-size-fits-all solution, researchers should select metrics based on their specific objectives.

### 5.3 What is the importance of fairness metrics in generative models?

Generative models-based synthetic data can inherit biases from the algorithms used to learn from real-world training data [22]. Some researchers have explored bias for facial applications, such as inaccuracies from race or gender bias [98] or reduced utility in text recognition due to repetitive words [91]. Fairness in synthetic data involves recognizing and rectifying biases in training data and algorithms to avoid discriminating against certain groups. While researchers have explored the potential of fairness metrics to handle bias in synthetic data [98], Cheng et al. [23] have analyzed the significance of fairness metrics in downstream performance. In downstream tasks, researchers rely on application-specific metrics. However, depending on these metrics can lead to overfitting specific tasks while failing to capture the broader distribution of real data. Fairness metrics can help capture underlying distributions across various groups. Therefore, there is still room for significant contribution to fairness in generative models, such as fairness metrics [98], debiasing techniques [28], or counterfactual fairness [2].

## 6 Acknowledgments

This work was supported by the Alan Turing Institute under the Turing/Accenture strategic partnership grant R-AST-040.

## References

- [1] Martin Abadi, Andy Chu, Ian Goodfellow, H. Brendan McMahan, Ilya Mironov, Kunal Talwar, and Li Zhang. Deep Learning with Differential Privacy. In *Proceedings of the 2016 ACM SIGSAC Conference on Computer and Communications Security*, pages 308–318, Vienna Austria, October 2016. ACM.
- [2] Mahed Abroshan, Mohammad Mahdi Khalili, and Andrew Elliott. Counterfactual Fairness in Synthetic Data Generation. In *NeurIPS 2022 Workshop on Synthetic Data for Empowering ML Research*, New Orleans, U.S., October 2022.

- [3] Gergely Acs, Luca Melis, Claude Castelluccia, and Emiliano De Cristofaro. Differentially Private Mixture of Generative Neural Networks. In *2017 IEEE International Conference on Data Mining (ICDM)*, pages 715–720, New Orleans, LA, November 2017. IEEE.
- [4] Suzan Ece Ada, Emre Ugur, and H. Levent Akin. Generalization in Transfer Learning. *Robotica*, 40(11):3811–3836, November 2022. arXiv:1909.01331 [cs, stat].
- [5] Moustafa Alzantot and Mani Srivastava. Differential privacy synthetic data generation using WGANs, 2019. original-date: 2019-05-29T04:58:58Z.
- [6] Martin Arjovsky, Soumith Chintala, and Léon Bottou. Wasserstein Generative Adversarial Networks. In *Proceedings of the 34th International Conference on Machine Learning*, pages 214–223, Sydney, Australia, July 2017. PMLR. ISSN: 2640-3498.
- [7] J. Scott Armstrong and Fred Collopy. Error measures for generalizing about forecasting methods: Empirical comparisons. *International Journal of Forecasting*, 8(1):69–80, June 1992.
- [8] Maryam Azadmanesh, Behrouz Shahgholi Ghahfarokhi, and Maede Ashouri Talouki. A White-Box Generator Membership Inference Attack Against Generative Models. In *2021 18th International ISC Conference on Information Security and Cryptology (ISCISC)*, pages 13–17, Iran, September 2021. IEEE (Institute of Electrical and Electronics Engineers. ISSN: 2475-2371.
- [9] Eugene Bagdasaryan, Omid Poursaeed, and Vitaly Shmatikov. Differential Privacy Has Disparate Impact on Model Accuracy. In *Advances in Neural Information Processing Systems*, volume 32, Vancouver, Canada, 2019. Curran Associates, Inc.
- [10] Brett K. Beaulieu-Jones, Zhiwei Steven Wu, Chris Williams, Ran Lee, Sanjeev P. Bhavnani, James Brian Byrd, and Casey S. Greene. Privacy-preserving generative deep neural networks support clinical data sharing. *American Heart Association*, 12(7):e005122, 2019.
- [11] Steven M Bellovin, Preetam K Dutta, and Nathan Reiter. Privacy and synthetic datasets. *Stan. Tech. L. Rev.*, 22:1, 2019.
- [12] Daniel Bernau, Jonas Robl, and Florian Kerschbaum. Assessing Differentially Private Variational Autoencoders Under Membership Inference. In Shamik Sural and Haibing Lu, editors, *Data and Applications Security and Privacy XXXVI*, Lecture Notes in Computer Science, pages 3–14, Cham, 2022. Springer International Publishing.
- [13] Alex Bie, Gautam Kamath, and Guojun Zhang. Private GANs, Revisited. *Transactions on Machine Learning Research*, February 2023.
- [14] Umanga Bista, Alexander Mathews, Aditya Menon, and Lexing Xie. SupMMD: A Sentence Importance Model for Extractive Summarization using Maximum Mean Discrepancy. In Trevor Cohn, Yulan He, and Yang Liu, editors, *Findings of the Association for Computational Linguistics: EMNLP 2020*, pages 4108–4122, Online, November 2020. Association for Computational Linguistics.
- [15] Zhipeng Cai, Zuobin Xiong, Honghui Xu, Peng Wang, Wei Li, and Yi Pan. Generative Adversarial Networks: A Survey Toward Private and Secure Applications. *ACM Computing Surveys*, 54(6):132:1–132:38, July 2021.
- [16] Dingfan Chen, Tribhuvanesh Orekondy, and Mario Fritz. GS-WGAN: a gradient-sanitized approach for learning differentially private generators. In *Proceedings of the 34th International Conference on Neural Information Processing Systems, NIPS’20*, pages 12673–12684, Red Hook, NY, USA, December 2020. Curran Associates Inc.
- [17] Dingfan Chen, Ning Yu, Yang Zhang, and Mario Fritz. GAN-Leaks: A Taxonomy of Membership Inference Attacks against Generative Models. In *Proceedings of the 2020 ACM SIGSAC Conference on Computer and Communications Security*, pages 343–362, Virtual Event USA, October 2020. ACM.
- [18] Dongjie Chen, Sen-ching Samson Cheung, Chen-Nee Chuah, and Sally Ozonoff. Differentially Private Generative Adversarial Networks with Model Inversion. In *2021 IEEE International Workshop on Information Forensics and Security (WIFS)*, pages 1–6, Montpellier, France, December 2021. IEEE. ISSN: 2157-4774.
- [19] Hsin-Yi Chen and Szu-Hao Huang. Generating a trading strategy in the financial market from sensitive expert data based on the privacy-preserving generative adversarial imitation network. *Neurocomputing*, 500:616–631, August 2022.
- [20] Jiawei Chen, Janusz Konrad, and Prakash Ishwar. VGAN-Based Image Representation Learning for Privacy-Preserving Facial Expression Recognition. In *2018 IEEE/CVF Conference on Computer Vision and Pattern Recognition Workshops (CVPRW)*, pages 1651–165109, Salt Lake City, UT, USA, June 2018. IEEE.



- [21] Junjie Chen, Wendy Hui Wang, Hongchang Gao, and Xinghua Shi. PAR-GAN: Improving the Generalization of Generative Adversarial Networks Against Membership Inference Attacks. In *Proceedings of the 27th ACM SIGKDD Conference on Knowledge Discovery & Data Mining*, pages 127–137, Virtual Event Singapore, August 2021. ACM.
- [22] Tianwei Chen, Yusuke Hirota, Mayu Otani, Noa Garcia, and Yuta Nakashima. Would Deep Generative Models Amplify Bias in Future Models? In *Proceedings of the IEEE/CVF Conference on Computer Vision and Pattern Recognition*, pages 10833–10843, Seattle Convention Center, 2024. IEEE.
- [23] Victoria Cheng, Vinith M. Suriyakumar, Natalie Dullerud, Shalmali Joshi, and Marzyeh Ghassemi. Can You Fake It Until You Make It?: Impacts of Differentially Private Synthetic Data on Downstream Classification Fairness. In *Proceedings of the 2021 ACM Conference on Fairness, Accountability, and Transparency*, pages 149–160, Virtual Event Canada, March 2021. ACM.
- [24] Edward Choi, Siddharth Biswal, Bradley Malin, Jon Duke, Walter F Stewart, and Jimeng Sun. Generating multi-label discrete patient records using generative adversarial networks. In *Machine learning for healthcare conference*, pages 286–305, Boston, Massachusetts, USA, 2017. PMLR, PMLR.
- [25] William L. Croft, Jörg-Rüdiger Sack, and Wei Shi. Differentially private facial obfuscation via generative adversarial networks. *Future Generation Computer Systems*, 129:358–379, April 2022.
- [26] Jiankang Deng, Jia Guo, Niannan Xue, and Stefanos Zafeiriou. ArcFace: Additive Angular Margin Loss for Deep Face Recognition. In *Proceedings of the IEEE/CVF Conference on Computer Vision and Pattern Recognition*, pages 4690–4699, California, USA, 2019. IEEE.
- [27] Yonggui Dong, Zhaoyan Sun, and Huibo Jia. A cosine similarity-based negative selection algorithm for time series novelty detection. *Mechanical Systems and Signal Processing*, 20(6):1461–1472, August 2006.
- [28] Barbara Draghi, Zhenchen Wang, Puja Myles, and Allan Tucker. Identifying and handling data bias within primary healthcare data using synthetic data generators. *Heliyon*, 10(2):e24164, January 2024.
- [29] Cynthia Dwork. Differential Privacy: A Survey of Results. In Manindra Agrawal, Dingzhu Du, Zhenhua Duan, and Angsheng Li, editors, *Theory and Applications of Models of Computation*, Lecture Notes in Computer Science, pages 1–19, Berlin, Heidelberg, 2008. Springer.
- [30] Liyue Fan. A survey of differentially private generative adversarial networks. In *The AAAI Workshop on Privacy-Preserving Artificial Intelligence*, page 8, New York, USA, 2020.
- [31] T. Foss, E. Stensrud, B. Kitchenham, and I. Myrvtveit. A simulation study of the model evaluation criterion MMRE. *IEEE Transactions on Software Engineering*, 29(11):985–995, November 2003.
- [32] Matt Fredrikson, Somesh Jha, and Thomas Ristenpart. Model Inversion Attacks that Exploit Confidence Information and Basic Countermeasures. In *Proceedings of the 22nd ACM SIGSAC Conference on Computer and Communications Security, CCS '15*, pages 1322–1333, New York, NY, USA, October 2015. Association for Computing Machinery.
- [33] Lorenzo Frigerio, Anderson Santana de Oliveira, Laurent Gomez, and Patrick Duverger. Differentially Private Generative Adversarial Networks for Time Series, Continuous, and Discrete Open Data. In Gurpreet Dhillon, Fredrik Karlsson, Karin Hedström, and André Zúquete, editors, *ICT Systems Security and Privacy Protection, IFIP Advances in Information and Communication Technology*, pages 151–164, Cham, 2019. Springer International Publishing.
- [34] Oran Gafni, Lior Wolf, and Yaniv Taigman. Live Face De-Identification in Video. In *Proceedings of the IEEE/CVF International Conference on Computer Vision*, pages 9378–9387, Seattle, Washington, USA, 2019. IEEE.
- [35] Georgi Ganev. DP-SGD vs PATE: Which Has Less Disparate Impact on GANs?, November 2021.
- [36] Georgi Ganev, Bristena Oprisanu, and Emiliano De Cristofaro. Robin Hood and Matthew Effects: Differential Privacy Has Disparate Impact on Synthetic Data. In *Proceedings of the 39th International Conference on Machine Learning*, pages 6944–6959, Baltimore, Maryland, USA, June 2022. PMLR.
- [37] Georgi Ganev, Kai Xu, and Emiliano De Cristofaro. Graphical vs. Deep Generative Models: Measuring the Impact of Differentially Private Mechanisms and Budgets on Utility, May 2023.
- [38] Matteo Giomi, Franziska Boenisch, Christoph Wehmeyer, and Borbála Tasnádi. A Unified Framework for Quantifying Privacy Risk in Synthetic Data. *Proceedings on Privacy Enhancing Technologies*, 2023:312–328, 2023.
- [39] Andre Goncalves, Priyadip Ray, Braden Soper, Jennifer Stevens, Linda Coyle, and Ana Paula Sales. Generation and evaluation of synthetic patient data. *BMC Medical Research Methodology*, 20(1):108, May 2020.

- [40] Ian Goodfellow, Jean Pouget-Abadie, Mehdi Mirza, Bing Xu, David Warde-Farley, Sherjil Ozair, Aaron Courville, and Yoshua Bengio. Generative adversarial networks. *Communications of the ACM*, 63(11):139–144, October 2020.
- [41] Ishaan Gulrajani, Faruk Ahmed, Martin Arjovsky, Vincent Dumoulin, and Aaron C Courville. Improved training of wasserstein gans. *Advances in neural information processing systems*, 30, 2017.
- [42] Mehmet Emre Gursoy, Ling Liu, Stacey Truex, Lei Yu, and Wenqi Wei. Utility-Aware Synthesis of Differentially Private and Attack-Resilient Location Traces. In *Proceedings of the 2018 ACM SIGSAC Conference on Computer and Communications Security*, pages 196–211, Toronto Canada, October 2018. ACM.
- [43] Chunling Han and Rui Xue. Differentially private GANs by adding noise to Discriminator’s loss. *Computers & Security*, 107:102322, August 2021.
- [44] Jamie Hayes, Luca Melis, George Danezis, and Emiliano De Cristofaro. LOGAN: Membership Inference Attacks Against Generative Models. *Proceedings on Privacy Enhancing Technologies*, 2019(1):133–152, January 2019.
- [45] Martin Heusel, Hubert Ramsauer, Thomas Unterthiner, Bernhard Nessler, and Sepp Hochreiter. GANs Trained by a Two Time-Scale Update Rule Converge to a Local Nash Equilibrium, January 2018. arXiv:1706.08500 [cs, stat].
- [46] Benjamin Hilprecht, Martin Härterich, and Daniel Bernau. Monte carlo and reconstruction membership inference attacks against generative models. *Proc. Priv. Enhancing Technol.*, 2019(4):232–249, 2019.
- [47] Stella Ho, Youyang Qu, Bruce Gu, Longxiang Gao, Jianxin Li, and Yong Xiang. DP-GAN: Differentially private consecutive data publishing using generative adversarial nets. *Journal of Network and Computer Applications*, 185:103066, July 2021.
- [48] Florimond Houssiau, James Jordon, Samuel N. Cohen, Owen Daniel, Andrew Elliott, James Geddes, Callum Mole, Camila Rangel-Smith, and Lukasz Szpruch. TAPAS: a Toolbox for Adversarial Privacy Auditing of Synthetic Data. In *NeurIPS 2022 Workshop on Synthetic Data for Empowering ML Research*, New Orleans, Louisiana, USA, October 2022.
- [49] Aoting Hu, Renjie Xie, Zhigang Lu, Aiqun Hu, and Minhui Xue. TableGAN-MCA: Evaluating Membership Collisions of GAN-Synthesized Tabular Data Releasing. In *Proceedings of the 2021 ACM SIGSAC Conference on Computer and Communications Security, CCS ’21*, pages 2096–2112, New York, NY, USA, November 2021. Association for Computing Machinery.
- [50] Hailong Hu and Jun Pang. Model Extraction and Defenses on Generative Adversarial Networks, January 2021.
- [51] Jihyeon Hyeong, Jayoung Kim, Noseong Park, and Sushil Jajodia. An Empirical Study on the Membership Inference Attack against Tabular Data Synthesis Models. In *Proceedings of the 31st ACM International Conference on Information & Knowledge Management, CIKM ’22*, pages 4064–4068, New York, NY, USA, October 2022. Association for Computing Machinery.
- [52] Sana Imtiaz, Muhammad Arsalan, Vladimir Vlassov, and Ramin Sadre. Synthetic and Private Smart Health Care Data Generation using GANs. In *2021 International Conference on Computer Communications and Networks (ICCCN)*, pages 1–7, Athens, Greece, July 2021. IEEE.
- [53] Dihong Jiang, Guojun Zhang, Mahdi Karami, Xi Chen, Yunfeng Shao, and Yaoliang Yu. DP<sup>2</sup>-VAE: Differentially Private Pre-trained Variational Autoencoders, August 2022.
- [54] Tian Jin, Michael Carbin, Dan Roy, Jonathan Frankle, and Gintare Karolina Dziugaite. Pruning’s Effect on Generalization Through the Lens of Training and Regularization. *Advances in Neural Information Processing Systems*, 35:37947–37961, December 2022.
- [55] James Jordon, Jinsung Yoon, and Mihaela van der Schaar. PATE-GAN: Generating Synthetic Data with Differential Privacy Guarantees. In *ICLR 2019*, New Orleans, LA, USA, February 2022.
- [56] Tero Karras, Timo Aila, Samuli Laine, and Jaakko Lehtinen. Progressive Growing of GANs for Improved Quality, Stability, and Variation, February 2018. arXiv:1710.10196 [cs, stat].
- [57] Tero Karras, Samuli Laine, and Timo Aila. A style-based generator architecture for generative adversarial networks. In *Proceedings of the IEEE/CVF conference on computer vision and pattern recognition*, pages 4401–4410, California, USA, 2019. IEEE.
- [58] Jayoung Kim, Jinsung Jeon, Jaehoon Lee, Jihyeon Hyeong, and Noseong Park. OCT-GAN: Neural ODE-based Conditional Tabular GANs. In *Proceedings of the Web Conference 2021, WWW ’21*, pages 1506–1515, New York, NY, USA, June 2021. Association for Computing Machinery.
- [59] Diederik P Kingma and Max Welling. Stochastic gradient vb and the variational auto-encoder. In *Second International Conference on Learning Representations, ICLR*, volume 19, page 121, Alberta, Canada, 2014.

- [60] Anantaa Kotal, Aritran Piplai, Sai Sree Laya Chukkapalli, and Anupam Joshi. PriveTAB: Secure and Privacy-Preserving sharing of Tabular Data. In *Proceedings of the 2022 ACM on International Workshop on Security and Privacy Analytics, IWSPA '22*, pages 35–45, New York, NY, USA, April 2022. Association for Computing Machinery.
- [61] Zhenzhong Kuang, Zhiqiang Guo, Jinglong Fang, Jun Yu, Noboru Babaguchi, and Jianping Fan. Unnoticeable synthetic face replacement for image privacy protection. *Neurocomputing*, 457:322–333, October 2021.
- [62] Aditya Kunar, Robert Birke, Zilong Zhao, and Lydia Chen. DTGAN: Differential Private Training for Tabular GANs, July 2021.
- [63] JAEHOON LEE, Jiyeon Hyeong, Jinsung Jeon, Noseong Park, and Jihoon Cho. Invertible Tabular GANs: Killing Two Birds with One Stone for Tabular Data Synthesis. In *Advances in Neural Information Processing Systems*, volume 34, pages 4263–4273, online, 2021. Curran Associates, Inc.
- [64] Christophe Leys, Christophe Ley, Olivier Klein, Philippe Bernard, and Laurent Licata. Detecting outliers: Do not use standard deviation around the mean, use absolute deviation around the median. *Journal of Experimental Social Psychology*, 49(4):764–766, July 2013.
- [65] Jin Li. Assessing the accuracy of predictive models for numerical data: Not  $r$  nor  $r^2$ , why not? Then what? *PLOS ONE*, 12(8):e0183250, August 2017.
- [66] Yuancheng Li, Yimeng Wang, and Daoxing Li. Privacy-preserving lightweight face recognition. *Neurocomputing*, 363(C):212–222, October 2019.
- [67] Kang Liu, Benjamin Tan, and Siddharth Garg. Subverting Privacy-Preserving GANs: Hiding Secrets in Sanitized Images. *Proceedings of the AAAI Conference on Artificial Intelligence*, 35(17):14849–14856, May 2021.
- [68] Kin Sum Liu, Chaowei Xiao, Bo Li, and Jie Gao. Performing Co-membership Attacks Against Deep Generative Models. In *2019 IEEE International Conference on Data Mining (ICDM)*, pages 459–467, Beijing, China, November 2019. IEEE.
- [69] Yi Liu, Jialiang Peng, James J.Q. Yu, and Yi Wu. PPGAN: Privacy-Preserving Generative Adversarial Network. In *2019 IEEE 25th International Conference on Parallel and Distributed Systems (ICPADS)*, pages 985–989, Tianjin, China, December 2019. IEEE.
- [70] Yunhui Long, Boxin Wang, Zhuolin Yang, Bhavya Kailkhura, Aston Zhang, Carl Gunter, and Bo Li. G-PATE: Scalable Differentially Private Data Generator via Private Aggregation of Teacher Discriminators. In *Advances in Neural Information Processing Systems*, volume 34, pages 2965–2977, online, 2021. Curran Associates, Inc.
- [71] Pei-Hsuan Lu and Chia-Mu Yu. POSTER: A Unified Framework of Differentially Private Synthetic Data Release with Generative Adversarial Network. In *Proceedings of the 2017 ACM SIGSAC Conference on Computer and Communications Security*, pages 2547–2549, Dallas Texas USA, October 2017. ACM.
- [72] Yingzhou Lu, Minjie Shen, Huazheng Wang, Xiao Wang, Capucine van Rechem, Tianfan Fu, and Wenqi Wei. Machine Learning for Synthetic Data Generation: A Review, May 2024. arXiv:2302.04062 [cs].
- [73] Chuan Ma, Jun Li, Ming Ding, Bo Liu, Kang Wei, Jian Weng, and H. Vincent Poor. RDP-GAN: A Rényi-differential privacy based generative adversarial network. *IEEE Transactions on Dependable and Secure Computing*, 20(6):1–15, 2023. Conference Name: IEEE Transactions on Dependable and Secure Computing.
- [74] Maxim Maximov, Ismail Elezi, and Laura Leal-Taixé. CIAGAN: Conditional Identity Anonymization Generative Adversarial Networks. In *2020 IEEE/CVF Conference on Computer Vision and Pattern Recognition (CVPR)*, pages 5446–5455, Seattle, Washington, USA, June 2020. IEEE. ISSN: 2575-7075.
- [75] Sarina Meyer, Pascal Tilli, Pavel Denisov, Florian Lux, Julia Koch, and Ngoc Thang Vu. Anonymizing Speech with Generative Adversarial Networks to Preserve Speaker Privacy. In *2022 IEEE Spoken Language Technology Workshop (SLT)*, pages 912–919, Doha, Qatar, January 2023. IEEE.
- [76] Lu Mi, Macheng Shen, and Jingzhao Zhang. A Probe Towards Understanding GAN and VAE Models, December 2018. arXiv:1812.05676 [cs, stat].
- [77] Ilya Mironov. Rényi Differential Privacy. In *2017 IEEE 30th Computer Security Foundations Symposium (CSF)*, pages 263–275, California, USA, August 2017. IEEE. ISSN: 2374-8303.
- [78] Mehdi Mirza and Simon Osindero. Conditional Generative Adversarial Nets, November 2014. arXiv:1411.1784 [cs, stat].
- [79] Takeru Miyato, Toshiki Kataoka, Masanori Koyama, and Yuichi Yoshida. Spectral Normalization for Generative Adversarial Networks. In *Sixth International Conference on Learning Representations, ICLR*, Vancouver Convention Centre, Vancouver, Canada, February 2018.

- [80] Helena Montenegro, Wilson Silva, and Jaime S. Cardoso. Privacy-Preserving Generative Adversarial Network for Case-Based Explainability in Medical Image Analysis. *IEEE Access*, 9:148037–148047, 2021.
- [81] Vaikkunth Mugunthan, Vignesh Gokul, Lalana Kagal, and Shlomo Dubnov. DPD-InfoGAN: Differentially Private Distributed InfoGAN. In *Proceedings of the 1st Workshop on Machine Learning and Systems*, pages 1–6, Online United Kingdom, April 2021. ACM.
- [82] Sumit Mukherjee, Yixi Xu, Anusua Trivedi, Nabajyoti Patowary, and Juan L. Ferres. privGAN: Protecting GANs from membership inference attacks at low cost to utility. *Proceedings on Privacy Enhancing Technologies*, 2021(3):142–163, July 2021.
- [83] Peter Olukanmi, Fulufhelo Nelwamondo, Tshilidzi Marwala, and Bhekisipho Twala. Automatic detection of outliers and the number of clusters in k-means clustering via Chebyshev-type inequalities. *Neural Computing and Applications*, 34(8):5939–5958, April 2022.
- [84] Bristena Oprisanu, Georgi Ganev, and Emiliano De Cristofaro. On Utility and Privacy in Synthetic Genomic Data. In *Proceedings 2022 Network and Distributed System Security Symposium*, San Diego, CA, USA, April 2022. Internet Society.
- [85] Ke Pan, Maoguo Gong, and Yuan Gao. Privacy-enhanced generative adversarial network with adaptive noise allocation. *Knowledge-Based Systems*, 272:110576, July 2023.
- [86] Nicolas Papernot, Shuang Song, Ilya Mironov, Ananth Raghunathan, Kunal Talwar, and Ulfar Erlingsson. Scalable Private Learning with PATE. In *The Sixth International Conference on Learning Representations*, Vancouver, British Columbia, Canada, February 2018.
- [87] Cheolhee Park, Youngsoo Kim, Jong-Geun Park, Dowon Hong, and Changho Seo. Evaluating Differentially Private Generative Adversarial Networks Over Membership Inference Attack. *IEEE Access*, 9:167412–167425, 2021.
- [88] Noseong Park, Mahmoud Mohammadi, Kshitij Gorde, Sushil Jajodia, Hongkyu Park, and Youngmin Kim. Data synthesis based on generative adversarial networks. *Proceedings of the VLDB Endowment*, 11(10):1071–1083, June 2018.
- [89] Alec Radford, Luke Metz, and Soumith Chintala. Unsupervised representation learning with deep convolutional generative adversarial networks, 2016.
- [90] Tim Salimans, Ian Goodfellow, Wojciech Zaremba, Vicki Cheung, Alec Radford, Xi Chen, and Xi Chen. Improved Techniques for Training GANs. In *Advances in Neural Information Processing Systems*, volume 29, Barcelona, Spain, 2016. Curran Associates, Inc.
- [91] Taisho Sasada, Masataka Kawai, Yuzo Taenaka, Doudou Fall, and Youki Kadobayashi. Differentially-Private Text Generation via Text Preprocessing to Reduce Utility Loss. In *2021 International Conference on Artificial Intelligence in Information and Communication (ICAIC)*, pages 042–047, Jeju Island, Korea (South), April 2021. IEEE.
- [92] Florian Schroff, Dmitry Kalenichenko, and James Philbin. FaceNet: A unified embedding for face recognition and clustering. pages 815–823, June 2015.
- [93] Reza Shokri, Marco Stronati, Congzheng Song, and Vitaly Shmatikov. Membership inference attacks against machine learning models. In *2017 IEEE symposium on security and privacy (SP)*, pages 3–18, California, USA, 2017. IEEE.
- [94] Theresa Stadler, Bristena Oprisanu, and Carmela Troncoso. Synthetic Data – Anonymisation Groundhog Day. In *31st USENIX Security Symposium (USENIX Security 22)*, pages 1451–1468, Massachusetts, USA, 2022.
- [95] Hui Sun, Tianqing Zhu, Zhiqiu Zhang, Dawei Jin, Ping Xiong, and Wanlei Zhou. Adversarial Attacks Against Deep Generative Models on Data: A Survey. *IEEE Transactions on Knowledge and Data Engineering*, 35(4):3367–3388, April 2023.
- [96] Shun Takagi, Tsubasa Takahashi, Yang Cao, and Masatoshi Yoshikawa. P3GM: Private High-Dimensional Data Release via Privacy Preserving Phased Generative Model. In *2021 IEEE 37th International Conference on Data Engineering (ICDE)*, pages 169–180, Chania, Greece, April 2021. IEEE.
- [97] Uthaiapon Tao Tantipongpipat, Chris Waites, Digvijay Boob, Amaresh Ankit Siva, and Rachel Cummings. Differentially Private Synthetic Mixed-Type Data Generation For Unsupervised Learning. In *2021 12th International Conference on Information, Intelligence, Systems & Applications (IISA)*, pages 1–9, Chania Crete, Greece, July 2021. IEEE.
- [98] Huan Tian, Tianqing Zhu, and Wanlei Zhou. Fairness and privacy preservation for facial images: GAN-based methods. *Computers & Security*, 122:102902, November 2022.

- [99] Amirsina Torfi, Edward A. Fox, and Chandan K. Reddy. Differentially private synthetic medical data generation using convolutional GANs. *Information Sciences*, 586:485–500, March 2022.
- [100] Reihaneh Torkzadehmahani, Peter Kairouz, and Benedict Paten. DP-CGAN: Differentially Private Synthetic Data and Label Generation. In *2019 IEEE/CVF Conference on Computer Vision and Pattern Recognition Workshops (CVPRW)*, pages 98–104, Long Beach, CA, USA, June 2019. IEEE.
- [101] Isabel Wagner and David Eckhoff. Technical Privacy Metrics: A Systematic Survey. *ACM Computing Surveys*, 51(3):1–38, May 2019.
- [102] Ryan Webster, Julien Rabin, Loic Simon, and Frederic Jurie. Generating Private Data Surrogates for Vision Related Tasks. In *2020 25th International Conference on Pattern Recognition (ICPR)*, pages 263–269, Milan, Italy, January 2021. IEEE.
- [103] Yunqian Wen, Bo Liu, Ming Ding, Rong Xie, and Li Song. IdentityDP: Differential private identification protection for face images. *Neurocomputing*, 501:197–211, August 2022.
- [104] Kwan Yeung Wong and Fu-lai Chung. Visualizing Time Series Data with Temporal Matching Based t-SNE. In *2019 International Joint Conference on Neural Networks (IJCNN)*, pages 1–8, Budapest, Hungary, July 2019. ISSN: 2161-4407.
- [105] Liyang Xie, Kaixiang Lin, Shu Wang, Fei Wang, and Jiayu Zhou. Differentially Private Generative Adversarial Network, February 2018. arXiv:1802.06739 [cs, stat].
- [106] Chugui Xu, Ju Ren, Deyu Zhang, Yaoyue Zhang, Zhan Qin, and Kui Ren. GANobfuscator: Mitigating Information Leakage Under GAN via Differential Privacy. *IEEE Transactions on Information Forensics and Security*, 14(9):2358–2371, September 2019.
- [107] Depeng Xu, Shuhan Yuan, Lu Zhang, and Xintao Wu. FairGAN: Fairness-aware Generative Adversarial Networks. In *2018 IEEE International Conference on Big Data (Big Data)*, pages 570–575, Seattle, Washington, USA, December 2018.
- [108] Lei Xu, Maria Skoularidou, Alfredo Cuesta-Infante, and Kalyan Veeramachaneni. Modeling tabular data using conditional gan. *Advances in Neural Information Processing Systems*, 32:7335 – 7345, 2019.
- [109] Andrew Yale, Saloni Dash, Ritik Dutta, Isabelle Guyon, Adrien Pavao, and Kristin P. Bennett. Generation and evaluation of privacy preserving synthetic health data. *Neurocomputing*, 416:244–255, November 2020.
- [110] Ren Yang, Xuebin Ma, Xiangyu Bai, and Xiangdong Su. Differential Privacy Images Protection Based on Generative Adversarial Network. In *2020 IEEE 19th International Conference on Trust, Security and Privacy in Computing and Communications (TrustCom)*, pages 1688–1695, Guangzhou, China, December 2020. IEEE. ISSN: 2324-9013.
- [111] Jinsung Yoon, Lydia N. Drumright, and Mihaela van der Schaar. Anonymization Through Data Synthesis Using Generative Adversarial Networks (ADS-GAN). *IEEE Journal of Biomedical and Health Informatics*, 24(8):2378–2388, August 2020.
- [112] Chenhan Zhang, Shui Yu, Zhiyi Tian, and James J. Q. Yu. Generative Adversarial Networks: A Survey on Attack and Defense Perspective. *ACM Comput. Surv.*, 56(4):91:1–91:35, November 2023.
- [113] Wei Zhang, Brian Barr, and John Paisley. Understanding Counterfactual Generation using Maximum Mean Discrepancy. In *Proceedings of the Third ACM International Conference on AI in Finance, ICAIF ’22*, pages 44–52, New York, NY, USA, October 2022. Association for Computing Machinery.
- [114] Zhongqiang Zhang, Ge Liu, Fuhuan Cai, Duo Liu, and Xiangzhong Fang. Boosting domain generalization by domain-aware knowledge distillation. *Knowledge-Based Systems*, 280:111021, November 2023.
- [115] Ziqi Zhang, Chao Yan, and Bradley A. Malin. Membership inference attacks against synthetic health data. *Journal of Biomedical Informatics*, 125:103977, January 2022.
- [116] Zilong Zhao, Aditya Kunar, Robert Birke, Hiek Van der Scheer, and Lydia Y. Chen. CTAB-GAN+: enhancing tabular data synthesis. *Frontiers in Big Data*, 6, January 2024.
- [117] Junhao Zhou, Yufei Chen, Chao Shen, and Yang Zhang. Property Inference Attacks Against GANs. In *NDSS 2022*, San Diego, California, April 2022.
- [118] Cheng Zhuo, Di Gao, and Liangwei Liu. PKDGAN: Private Knowledge Distillation With Generative Adversarial Networks. *IEEE Transactions on Big Data*, pages 1–14, 2022.